UNIVERSITÀ
DEGLI STUDI
DI PADOVA

Sede Amministrativa: Università degli Studi di Padova

DIPARTIMENTO DI ISTOLOGIA, MICROBIOLOGIA E BIOTECNOLOGIE MEDICHE

SCUOLA DI DOTTORATO DI RICERCA IN BIOCHIMICA E BIOTECNOLOGIE
INDIRIZZO BIOTECNOLOGIE
CICLO: XXII

# A GENE NETWORK FOR HEAD ORGANIZER FORMATION

**Direttore della Scuola :** Ch.mo Prof. Giuseppe Zanotti

**Coordinatore d'indirizzo:** Ch.mo Prof. Giorgio Valle

**Supervisore** :Ch.mo Prof. Giorgio Bressan e Ch.mo Prof. Stefano Piccolo

**Dottorand**o : SANDRA MARIA SOLIGO

RIASSUNTO

**L'organizzatore di Spemann e' un tessuto con proprieta' uniche in quanto determina il piano corporeo dei vertebrati: la totalita' dei vari componenti tissutali, nelle giuste proporzioni e corretto posizionamento. Nonostante che i singoli "induttori" di testa e tronco siano stati identificati, il come questi si assemblino in modo coordinato (quantitativamente, spazialmente e temporalmente) rimane tuttora un mistero.**

**Per comprendere questo fenomeno, in questa tesi ci siamo concentrati sui meccanismi che stabiliscono l'architettura interna dello stesso organizzatore. Abbiamo trovato che l'attivita' di due ligandi, Nodal ed ADMP, realizza una rete genica che definisce un asse antero-posteriore in miniatura, localizzato nell'endoderma dorsale. Al polo posteriore di questo "asse", Nodal protegge l'induzione della testa competendo con ADMP per un recettore condiviso, ACVR2a; ADMP riesce ad agire solo molto piu'anteriormente, e nel fare questo, restringe le induzioni di Nodal. Questi segnali opposti riaggiustano la loro forza e dominio di azione in modo reciproco, attraverso feedback negativi e positivi. Cosi' facendo, i livelli di induttori della testa restano proporzionali ai segnali generali dal tronco e tamponati contro eventuali variazioni degli stessi. Nuovi elementi di regolazione sono essenziali in questa dinamica comunicazione; tra questi, un microRNA, miR-15/16, che garantisce robustezza alla formazione della testa.**

**In conclusione, qui proponiamo un modello che offre una spiegazione molecolare delle proprieta' dell'organizzatore di Spemann.**

**SUMMARY**

**The Spemann organizer determines the body plan, in its full variety of tissue components, normal proportion and placement. Although individual organizer's inducers responsible for head and trunk inductions have been identified, how these are handed out in perfect quantitative, spatial and temporal coordination remains enigmatic.**

**Here we focused on the mechanisms establishing the organizer own architecture as key to explain such signaling coordination. We found that a crosstalk between two ligands emanating from the trunk organizer, Nodal and ADMP, defines a miniature anteroposterior axis. At its posterior pole, Nodal protects head-induction by competing ADMP for a shared receptor, ACVR2a; ADMP is allowed to signal more anteriorly to restrain these inductions. These opposing signaling centers reciprocally adjust their strength and range of activity by multiple negative and positive loops. In so doing, the levels of head inducers remains proportional to signals generated in the trunk and buffered against their fluctuations. Several new regulatory elements are essential for this dynamic cross-talk, including a microRNA, miR-15/16, endowing robustness to head formation.**

**In sum, we propose a model that offers a molecular explanation for key properties of the Spemann's organizer.**

# INTRODUCTION

## XENOPUS AS A MODEL SYSTEM

With its rapid embryonic development, large egg size (1-2 mm in diameter) and high numbers of embryos (1,500 per female), *Xenopus* provides a favorable model system for the study of vertebrate development in particularly early embryogenesis.

The oocyte is radially symmetrical and is divided into an animal and a vegetal domain (Figure 1). The dorsal side of the amphibian embryo contains the information for the differentiation of many different cell types. The first external sign of asymmetry in the *Xenopus* egg after fertilization is the appearance of an unpigmented *dorsal crescent* (called the grey crescent in some amphibians), which is caused by a rotation of the egg cortical cytoplasm that is driven by microtubules. The dorsal crescent is formed opposite the sperm entry point, and it is the *first sign of asymmetry* in the zygote (Figure 1).

As the embryo rapidly divides into smaller and smaller cells, without intervening growth (i.e, cleavage stages), a cavity called the *blastocoel* is formed, which defines the blastula stage. By the late blastula stage (9 h of development), the *three germ layers* become defined. The ectoderm, or animal cap, forms the roof of the blastocoel. The mesoderm is formed in a ring of cells in the marginal zone, located between the ectoderm and endoderm. At the *gastrula stage* (10 h), involution of the mesoderm towards the inside of the embryo starts at the dorsal blastopore lip. The morphogenetic movements of gastrulation lead to the formation of the vertebrate body plan, patterning the ectoderm, mesoderm and endoderm. Later on, the neural plate, or future central nervous system (CNS), becomes visible in dorsal ectoderm. By the tailbud stage (24-42 h), a larva with a neural tube located between the epidermis and the notochord has formed. The blastopore gives rise to the anus, and the mouth is generated by secondary perforation (Figure 1) (De Robertis et al., 2000).

## EARLY SIGNALING EVENTS

***WNT signaling*** (Figure 2). A breakthrough in the study of early dorsal side specification was the discovery that βcatenin is translocated into the nuclei of cells on

the dorsal side of the embryo at the early blastula stage. *Xenopus* βcatenin has been shown to be required for dorsal axis formation and loss of βcatenin inhibits axial development. βcatenin belongs to the Wnt signaling pathway and microinjection of Wnt, βcatenin or other positive mediators of this pathway leads to duplication of the whole body (siamese embryos) (Figure 2B) (De Robertis et al., 2000).

***Mesoderm induction by TGFβ signaling (by Nodal)*** (Figure 3)**.** The next step in dorsal-ventral axis formation is the induction of mesoderm. As shown in Figure 3, the asymmetry in βcatenin is translated into an asymmetry of another signaling pathway: TGFβ (Figure 4). TGFβ is a super-family of cytokines (>30 family members) with different functions during the embryonic development and the adult tissues homeostasis (De Robertis et al., 2000). The main TGFβ of the embryo is a cytokine called Nodal. Genetic and embryological evidences indicate that Nodal proteins have important functions in mesoderm formation in Xenopus and mammals.

***TGFβ/Nodal signal transduction*** (Figure 4). TGFβ uses a simple mechanism to signal to the target cell. Specific serin/treonin kinase receptors, type I and II, are assembled by ligand, generating tetrameric receptors ( two of each). In this complex, receptor type II activates receptor type I after phosphorylation of its GS region. Then receptor type I phosphorilates R-Smad proteins that transmit the signal (De Robertis et al., 2000, Niehrs, 2004). The type II receptor for Nodal is ACVR2.

R-Smad phosphorilation increases R-Smads affinity for a particular member of the family, Smad4. This protein (Smad4 or co-Smad) is requested to assemble an active transcriptional complex. The Smad complex accumulates in the nucleus and there it can interact with specific co factors, activators or repressors, which stabilize the interaction with target genes.

**THE FORMATION OF THE SPEMANN ORGANIZER**

As mentioned above, Nodal signaling is not even in the entire mesoderm: a dorsal peak level of Nodal activity (Figure 3) induces on the dorsal mesoderm the most fundamental player of early development: the Spemann-Mangold organizer tissue (Figure 5).

Indeed, eighty years ago, the “organizer” experiment by Spemann and Mangold demonstrated that a restricted group of cells of the embryo, the dorsal blastopore lip of

the amphibian gastrula, is endowed with extraordinary inducing activities (De Robertis, 2006; Harland and Gerhart, 1997; Niehrs, 2004; Spemann and Mangold, 2001). Grafted in an ectopic location of a host embryo, this tissue recruits neighboring cells to form a secondary body axis. Thoughtfully, Spemann and Mangold (1924) wrote that "*The term "organizer" - rather than, perhaps, "determiner" - is supposed to express the idea that the effect emanating from these preferential regions is not only determinative in a definite restrictive direction, but it possesses all the enigmatic peculiarities which are known to us only from living organisms*" (Spemann and Mangold, 2001). After decades, despite the identification of the key players used by the organizer to induce distinct tissue-types, what ultimately defines those *enigmatic peculiarities*, namely, the set of molecular instructions required to organize a perfectly patterned body plan, remains one of the unsolved mystery in developmental biology.

***The organizer as a source of antagonists.*** (Figure 6). The "inducer" molecules emitted by the organizer are secreted antagonists of growth factors: during gastrulation, gradients of these antagonists restrict cell fates by confining and dosing the activity of embryonic morphogens along the embryonic axes (De Robertis et al., 2000). So far, the best understood of these processes is the establishment of the dorso-ventral axis, organized by a gradient of BMP inhibitors (Chordin, Noggin, Follistatin) (Ben-Zvi et al., 2008; Inomata et al., 2008; Khokha et al., 2005; Piccolo et al., 1996; Reversade and De Robertis, 2005; Zimmerman et al., 1996).

Concomitantly, the Spemann's organizer patterns the embryo also along the antero-posterior axis. Key for this latter activity is the organizer internal patterning: distinct cell populations display different inducing properties, corresponding to the head and trunk organizers. Head-organizing activity require the concomitant repression of Wnt (i.e. by Dkk), Nodal (i.e. by Cerberus, Lefty) and BMP signaling, whereas the trunk organizer involves only repression of BMPs (Glinka et al., 1998; Glinka et al., 1997; Niehrs, 2004; Piccolo et al., 1999) (Figure 6).

## ROLE OF MicroRNAs IN EARLY SIGNALING AND ORGANIZER SPECIFICATION

The work presented in this thesis was initiated in an attempt to understand the role of microRNAs in Organizer function. Part of this work is published: it has been initiated

and carried out mainly by my colleagues Graziano Martello and Luca Zacchigna (Martello et al., 2007), with whom I collaborated. We have here summarized our key findings in Figure 9, as explained in the Results.

***microRNA biogenesis*** (Figure 7A). miRNAs are a universal and pervasive feature of animal and plant genomes; current estimates suggest that the human genome contains at least hundreds of distinct miRNAs potentially regulating a very large fraction of the transcriptome(Bartel, 2009; Bartel and Chen, 2004).

MicroRNAs are a class of 20-25 nucleotide (nt)-long non-coding RNAs that modulate gene expression through canonical base pairing between the "seed" sequence of the miRNA (nt 2-8 at the 5' of the miRNA) and its complementary "seed-match" sequence present in the 3'UTR of target mRNAs (Bartel, 2009). microRNAs have a peculiar biogenesis: they are first transcribed as part of longer precursors (pri-miRNA), that fold on themselves to form hairpin structures. pri-miRNAs are then processed in the nucleus by the Drosha complex, transported into the cytoplasm via exportin 5, where they undergo final processing by the Dicer ribonuclease (Carthew and Sontheimer, 2009). Mature miRNAs are rapidly unwounded to be incorporated in the RNA-induced silencing complex (RISC) by associating with Argonaute proteins. Within the RISC, the single-stranded miRNA guides target selection, causing inhibition of mRNA translation and/or stability (Brodersen and Voinnet, 2009; Carthew and Sontheimer, 2009).

***miRNAs and cell signaling.*** Inhibition of miRNA biogenesis (e.g., through ablation of Dicer) clearly reveals the essentiality of miRNAs for a wide array of biological processes, including control of proliferative homeostasis, differentiation or embryonic stemness(Murchison et al., 2005; Tang et al., 2007; Yi et al., 2008). However, uncovering the function of individual miRNAs is challenging. First, miRNAs are frequently present as families of redundant genes, complicating genetic dissections. Second, each miRNA displays a vast number of putative targets, covering disparate functions, with no means to decide *a priori* which one is most meaningful, and thus worthy experimental validation. Third, the degree of target downregulation imposed by miRNAs often tends to be quantitatively modest; thus, most proteins should remain effective over this degree of inhibition. These considerations suggest that despite most genes are predicted to be miRNA targets, only a fraction of these interactions will prove instrumental for overt biological responses and phenotypes.

As a resolution to this conundrum - rather than querying miRNA:target pairs to predict miRNA biological functions - the reverse question, asking what biological processes might represent prime candidates for miRNA-mediated regulation, may be productive. In this work, we have provided evidences in favor of miRNAs and signaling from Wnt and TGFβ growth factors.

Signaling complexes are indeed highly dynamic, ephemeral and non-stoichiometric molecular ensembles, translating into well-established dose-dependent responses. As such, they are the ideal targets for the degree of quantitative fluctuations imposed by miRNAs. This enables the multi-gene regulatory capacity of miRNAs to remodel the signaling landscape, facilitating or opposing the transmission of information to downstream effectors in an effective and timely manner(Tsang et al., 2007).

***microRNAs and biological robustness***. There has been in the last couple of years a great interest in microRNAs as mediators of biological robustness, that can be defined as the capacity of a biological system to be resilient and withstand to perturbations, genetic or environmental.

Theoretical work predicts that the dynamic kinetic properties of miRNAs are ideally suited to buffer fluctuation in gene networks as miRNAs may affect gene expression with shorter delay than transcriptional repression (Hornstein and Shomron, 2006; Li et al., 2009; Tsang et al., 2007).

Feedforward and feedback loops are recurrent signaling network motifs essential for correct gene expression and are also critical for robustness. Feedforward loops, for instance, ensure efficient transcriptional response to signals and allow rapid deactivation when the input shuts off (Milo et al., 2002; Shen-Orr et al., 2002); conversely, negative feedback loops are important for homeostasis, acting as stabilizing elements in gene expression (Alon, 2007).

In *Drosophila*, pioneering work from Cohen, Bartel and colleagues showed that miRNAs and their target mRNAs are expressed in a mutually-exclusive fashion, as judged for instance by in situ hybridization (Farh et al., 2005; Stark et al., 2005). This suggested that miRNAs participate in signaling networks to stabilize cell identity by repressing “leaky” target mRNAs in tissue where they should not be expressed. As such, miRNAs act as reinforcers and backups of tissue-specific transcriptional programs (Hornstein and Shomron, 2006; Tsang et al., 2007). This defines a coherent feedback

loop, whereby the miRNA and its target are oppositely regulated by the same signal (Figure 7B).

Although the logic of coherent loops is intuitive, this hardly exhausts the regulatory potential of miRNAs. New evidences are starting to paint a new picture, perhaps prevalent, of how miRNAs can shape signaling pathways. Genome-wide computational and transcriptome analyses showed that miRNAs are co-expressed with their targets, and this is particularly true for evolutionary conserved miRNA:target pairs (Martinez et al., 2008). This extends the functional importance of miRNAs to "incoherent" network topologies (Figure 7B), in which the miRNA and its target are coactivated (or corepressed) by the same signaling cues (Hornstein and Shomron, 2006). This design serves homeostasis to maintain steady-state levels of the target protein from unwanted signaling fluctuations (as the miRNA would tune the translation of its target in a direction opposite to that one the signal).

Despite these speculations, little experimental work has been carried out to sustain the notion of miRNA and Biological robustness and on miRNA in signaling networks. This thesis work represents a step forward in this direction.

## AIM OF THIS WORK: ADDRESSING UNSOLVED ISSUES IN SPEMANN'S ORGANIZER BIOLOGY

A wealth of embryological and genetic evidences indicates that head and trunk organizers are induced by the same upstream signals, that is, by the maximal intensity of βatenin and Nodal signaling on the future dorsal side (De Robertis et al., 2000; Martello et al., 2007). Similarly, in the mouse, Nodal/Smad4-dependent activity is essential both for formation of the Node and induction of the Anterior Visceral Endoderm, two tissues corresponding to head and trunk organizer tissues that only if combined together can recapitulate complete anteroposterior development upon transplantation into a host embryo (Tam and Loebel, 2007).

Thus, a question still requiring in depth dissection is what regulatory network first distinguishes and then coordinates the development of these two cell populations in a mutually dependent manner within the organizer territory.

Also unknown are the mechanisms that, after this initial subdivision has taken place, ensure reliable antero-posterior development. In principle, from what we know at the gene-network level, the patterning of the organizer should be all but robust, as little fluctuations in individual players would appear to have catastrophic consequences. For example, Nodal transcription is potently fostered by its own signaling (Norris et al., 2002; Osada et al., 2000) such that, before gastrulation, Nodal genes are expressed in the future organizer territory (Jones et al., 1995; Takahashi et al., 2000); what then prevents Nodal activity from expanding indefinitely? Conversely, Nodal also induces its own inhibitors Cerberus and Lefty that act redundantly to oppose mesoderm formation (Perea-Gomez et al., 2002; Piccolo et al., 1999). Thus, even minor deviations from the optimal equilibrium could potentially mount a "chain-reaction", putting at risk organizer formation. In contrast to such theoretical instability, perfect offspring are produced time after time.

***CONCLUSIONS OF THIS THESIS.*** The work here described was initiated to shed light on some of these questions. By means of in vivo experiments in *Xenopus* embryos we provide a system-level understanding of the dynamics of genes, microRNAs and protein interactions operating in organizer specification and highlights the design principles employed for embryonic self-regulation in antero-posterior patterning.

# RESULTS

**Wnt-βcatenin signaling and robustness in antero-posterior patterning**

Robustness is an imbued characteristic of living systems and can be defined as the capacity to resist to genetic or enviromental fluctuations to generate a reproducible outcome (at the whole body, tissue or cell level). Body patterning is an example of robustness; this trait must be embedded by the primary generator of "order" in the body, the Spemann organizer.

As maternal Wnt-βcatenin signaling is a primary step for the formation of the organizer (see introduction) (De Robertis et al., 2000), we first asked if the head and trunk components of the organizer are differentially affected by βcatenin fluctuations. For this, we injected anti-βcatenin morpholinos (MO) in Xenopus embryos at the 2-cell stage at different doses (from 4 to 60 ng) (Figure 8). Quantitative knockdown of βcatenin (class I embryos) leads to loss of embryonic antero-posterior and dorso-ventral polarities (Figure 8B and 8F); interestingly, however, partial loss of βcatenin (class II embryos) particularly affected head (as visualized by in situ hybridization for the anterior markers *RX1* and *XAG-1*, recognizing eye and cement gland, respectively (Figure 8C and 8G), rather than trunk development (note the remaining neural tube marker *Sox2* expression in Figure 8G); even milder depletions had no effects (class III embryos - Figure 8D and 8H). This suggests that head induction either represents a high threshold βcatenin response, or it is less robust (i.e., less able to self-regulate) than the gene network regulating trunk development.

**A microRNA relevant for the formation of the Spemann organizer**

As mentioned in the introduction, the mechanisms ensuring the reliable activity of the Spemann organizer are not understood; however, recent evidences that implied microRNAs as potential mediators of biological robustness attracted our attention (Hornstein and Shomron, 2006; Milo et al., 2002; Tsang et al., 2007).

Indeed, we recently identified a microRNA family downstream of βcatenin, miR-15/16, that limits the expression of the Nodal receptor ACVR2a (Martello et al., 2007). As shown in Figure 9 A and B, miR-15/16 biogenesis is inhibited by βcatenin (Figure 9A), leading to an accumulation of ACVR2a on the dorsal side (Figure 9B); this

contributes to the generation of the dorsal peak of Nodal signaling, locking in place organizer induction (Martello et al., 2007).

Biologically, miR-15/16 is essential to set the final size of the Organizer, as loss of this miRNA by microinjection of Xenopus embryos with anti-miR15/16 morpholinos causes an increased expression and expansion of organizer genes, as visualized by in situ hybridization (Figure 9C). This is a consequence of enhanced responsiveness to endogenous Nodal ligands as visualized by the 3-fold increase of a Smad reporter (Mix2-luciferase reporter) co-injected with anti-mir15/16 morpholinos, compared to control (Figure 9D).

**miR-15/16 confers robustness to Organizer function.**

In light of the link between miRNAs and robustness (see introduction): Is miR15/16 relevant to robustness for organizer development in an embryo facing perturbations in patterning signals such as βcatenin? We tested this hypothesis by comparing miR15/16 deficiency in control embryos and in embryos with reduced βcatenin signaling. In wild-type embryos, loss of miR-15/16 by injection of miR-15/16-MO leads to a mild anteriorized phenotype (as shown by the cement gland and eye markers *XAG-1* and *RX-1*, Figures 10A-B). This result is in line with miR-15/16 functioning as inhibitor of organizer gene expression, as shown above (Martello et al., 2007). Unexpectedly, however, miR-15/16 depletion in class III βcatenin morphants caused the *opposite* phenotype, namely, complete *loss* of head structures without affecting trunk development (Figures 10D, compare with 10B). Furthermore, raising the levels of the miR-15/16 target ACVR2a also effectively reduced head development in class III embryos (Figure 10E). Thus, miR-15/16 can serve as suppressor or inducer of anterior fates, balancing βcatenin fluctuations. This also unveils an hitherto unidentified pathway by which attenuation of ACVR2a signaling by miR-15/16 enhances robustness of head formation.

**miR-15/16 stabilizes head development by inhibiting ADMP/ACVR2a signaling**

We next asked the nature of the ACVR2a ligand that inhibits head formation in our experimental setting. An appealing candidate was ADMP, a BMP-type ligand paradoxically expressed in the Spemann Organizer (Dosch and Niehrs, 2000; Moos et

al., 1995). Yet, the functions of ADMP for antero-posterior patterning are less understood.

We therefore tested the possibility that miR-15/16 confer robustness to head development by inhibiting ADMP activity. As shown in Figure 10F, compound loss of ADMP and miR15/16 in class III βcatenin morphants rescues normal head development. Similar rescue were obtained substituting loss of miR-15/16 with gain of ACVR2a (Figure 10G). Thus, inhibition of ADMP signaling by miR-15/16 stabilizes head development buffering β-catenin fluctuations.

In light of these results, we then tested if ACVR2a serves as ADMP receptor. To assay for direct biochemical interaction, mature myc-tagged ADMP was produced in the conditioned media of transfected 293T cells and incubated with recombinant Fc-tagged soluble versions of AVCR2a, BMPR2 (type II receptors) and ALK2 (the ADMP type I receptor(Reversade and De Robertis, 2005)). As shown in Figure 11A, ADMP protein was co-purified with ACVR2a and ALK2, but not with BMPR2.

**ACVR2a is the ADMP receptor**

To determine whether AVCR2a serves as functionally relevant ADMP receptor, we depleted endogenous ACVR2a from HepG2 cells and monitored ADMP responsiveness using a synthetic Smad1/5 luciferase reporter (*ID1*-lux). As shown in Figure 11B, siRNA-mediated knockdown of ACVR2a abolishes ADMP responsiveness, an effect phenocopied by transfection of mature miR-15. Conversely, ADMP responsiveness was promoted after raising ACVR2a levels. A complementary set of experiments was carried out in *Xenopus* embryos, where inactivation of ACVR2a by microinjection of Dominant-Negative AVCR2a mRNA abolished ADMP responsiveness (Figure 11C).

**An head organizer territory**

In overexpression assays, the head is generated by a set of secreted inhibitors expressed in the deep endoderm in front of the dorsal mesoderm (trunk organizer) (see details in Figure 6). As marker of such putative "head organizer" we used the *Cerberus* expression domain (Bouwmeester et al., 1996; Glinka et al., 1998). As ADMP inhibits head formation, two possibilities existed: either ADMP inhibited the response of the ectoderm to head inducer or it inhibited the expression of the head inducer themselves.

Indeed, ADMP affected the head organizer territory as we found that ADMP is required and sufficient to control *Cerberus* (Figure 12A-D).

This result implied that ADMP should signal within the anterior endoderm/head organizer. To test this, we first visualized Smad1 activation by immunohistochemistry for Phospho-Smad1 (Figure12E and 12F), which was dependent on endogenous ADMP as for intensity and number of positive nuclei (Figure 12G). Second, as shown in Figure 12H, ADMP-dependent Smad1-transcriptional activity could be revealed by targeting *ID1*-lux reporter plasmid in the C1 blastomeres (from which the leading edge derives (Vodicka and Gerhart, 1995)).

**A model for organizer's internal regulation**

Data presented so far suggest that miR-15/16 support head development in embryos facing fluctuations in βcatenin levels, and that this function stems from the ability of miR-15/16 to down-regulate ADMP signaling through ACVR2a. Thus, the miR-15/16-ACVR2a pair regulates both head-inducing (Nodal-ACVR2a-Smad2/3) and head-repressing (ADMP-ACVR2a-Smad1/5) signals.

We pondered how a receptor serving two opposing ligands could confer robustness to head formation. A plausible model is shown in Figure 13A: here, two ligands emanating from the trunk organizer (in blue) diffuse in the anterior endoderm (yellow). They signal in this second territory (inducing and repressing Cerberus and, likely, the other head organizer genes) but at the same time compete for a shared receptor, ACVR2a, expressed in limited amounts. Conceivably, as ADMP inhibits head organizer formation it has to act only after Nodal induced it, suggesting a temporal dynamic in the two signals: first Nodal and then ADMP. This logic is supported by the fact that ADMP expression itself (as any Organizer genes) is downstream of Nodal (Martello et al., 2009). For ADMP to signal, however, the limitedness of ACVR2a imposes that ADMP must outcompete Nodal from binding to ACVR2a and take its place.

To test these ideas, we co-injected *Xnr1* mRNA (the main *Xenopus* Nodal ligand) and *ADMP* mRNAs and monitored their activity either on Smad1/5 (*ID1*-lux) or Smad2/3 (*Mix.2*-lux) reporters. As show in Figure 13B, ADMP activity was potently antagonized by Xnr1. This is unlikely to be caused by intracellular competition at the level of some signal transducer (i.e. Smad4), as raising the levels of ACVR2a by

injecting its mRNA effectively neutralized the inhibitory effect of Xnr1. In contrast, ADMP had no effects on the induction of the *Mix.2* promoter by Xnr1 (Figure 13C). This suggests that the endogenous amount of ACVR2a can indeed accommodate only a limited amount of ligands, as our model predicted. In contrast to our prediction, however, ADMP is never able to outcompete Nodal/Xnr1, as this binds ACVR2a more efficiently than ADMP.

**Two signaling centers within the organizer**

In sum, the requirement of the model was that ADMP should signal at levels that are comparable to those of Nodal in the anterior endoderm region. However, this constrain is hardly compatible with experimental data showing instead that Xnr1 is effective against ADMP, but not viceversa. As shown in Figure 14A, we reasoned that this requirement could be accounted for by considering the presence of Nodal antagonists, that is, Cerberus and Lefty expressed in the head organizer (Meno et al., 1999; Perea-Gomez et al., 2002; Piccolo et al., 1999). In the case of Cerberus, we used this gene as a mere read-out of the anterior endoderm tissue, without considering its biological function as extracellular inhibitor of Nodal (trapping it away from its receptor, Piccolo et al., 1999). Lefty operates through a similar mechanism, as it impedes Nodal-Receptor interaction by substituting nodal for interaction with its co-receptor Cripto (Wessely and DeRobertis, 2000).

We thus tested if the Nodal antagonists Cerberus and Lefty, by titrating Nodal away from ACVR2a, could set such receptor free for ADMP, allowing it to signal (Figure 14B). For this experiment, we monitored *Sizzled* expression as a well-characterized read-out of ADMP activity (Reversade and De Robertis, 2005). Injection of ADMP mRNA strongly cooperates with Nodal inhibition by *Cerberus-short* (*CerS*) mRNA (CerS is the pure Nodal inhibitory domain of Cerberus (Piccolo et al., 1999) (Figures 14C-E) Conversely, the activity of endogenous or ectopically expressed ADMP is opposed by the release of endogenous Nodal ligands in embryos depleted of endogenous *Cerberus/Lefty* (compare respectively Figure 14C with Figure 14E and Figure 14F with 14H). This validates the prediction that, within the organizer, Nodal antagonism sets ACVR2a receptor free for ADMP.

**Revealing head induction by the "head organizer-anterior endoderm"**

Together, the data indicate that the "head organizer" tissue defined by the expression of *Cerberus* is confined between two signaling centers, one in the trunk, defined by Nodal signaling and ADMP production, and a second one in the most anterior endoderm, set by Nodal antagonism and ADMP signaling serving as feedback inhibitor to attenuate expression of the head-inducing program (Figure 14A).

This prompted us to reinvestigate a long-standing paradox in embryology: if the anterior endoderm expresses head-inducing factors, why does it not induce ectopic heads when transplanted in recipient embryos (Bouwmeester et al., 1996; Schneider and Mercola, 1999; Tam and Steiner, 1999)? The model suggests a possible explanation for this conundrum: once explanted, the anterior endoderm is separated from the source of Nodal and ADMP (*Zig-Zag* symbol in Figure 15A), but still contains Cerberus protein. Before its onw transcriptional expression fades, this Cerberus protein traps and antagonizes any residual Nodal within the explant, leaving ADMP free to signal; this turns-off expression the head-inducers irreversibly. Indeed, we observed that *Cerberus* expression rapidly fades within minutes in isolated leading edge endoderm explants; in contrast, in the absence of ADMP, *Cerberus* remained expressed in these explants (Figure 15B). Remarkably, we found leading-edge endoderm depleted of ADMP, but not control explants, were able to induce anterior duplications including secondary heads (without ectopic trunk) once grafted in recipient embryos (Figures 15C and 15D). These findings validate the triple inhibitory model shown in Figure 14B and reveal the head organizing properties of the anterior endoderm.

# DISCUSSION

The Spemann Organizer stands out from other signaling centers of the embryo because of its widespread patterning effects. It defines development along the antero-posterior and dorso-ventral axes of the vertebrate body, mainly by secreting antagonists of growth factors of the WNT and TGFβ superfamilies. Qualitative models proposed more that a decade ago explain the organizer's region-specific inductions (i.e. head and trunk, dorsal and ventral) as the result of different combinations of antagonists (Niehrs, 2004). However, quantitative elements must be incorporated into this picture: antagonists define gradients of signals, rather than on-off switches, and, critically, the distinct poles of the embryo must constantly communicate with each other to ensure coordination, proportion and reliability in embryonic patterning. Such mutual exchange of positive and negative regulations (Figure 16A) should ultimately harmonize the relative levels and expression domains of distinct inducers. While the gene network establishing and tuning dorso-ventral patterning has been characterized, and is now even amenable to "system-biology" approaches (Barkai and Ben-Zvi, 2009; Ben-Zvi et al., 2008; Plouhinec and De Robertis, 2007), the program in place for antero-posterior regionalization is less understood.

**A self-regulating network to link head and trunk development**

In this work we have modeled the network of genes, miRNA and protein-protein interactions underlying the coordinated development of the head and trunk inducing centers of the Spemann organizer.

We started this work by asking if miR-15/16 could serve as a built-in safety system that oppose β-catenin fluctuations (either genetic or enviromentally caused). We found that miR-15/16 is a critical element downstream of β-catenin as common mediator of two opposing loops feeding on head-organizer gene expression (Figure 16B). In the coherent loop, β-catenin positively regulates Nodal expression directly as well as indirectly by inhibiting miR-15/16 production; this is overlaid by the incoherent miR-15 dependent regulation of ADMP signaling, serving as embedded self-inhibiting relay.

Our model does not advance on the combinations of signals and anti-signals by which the organizer determines head- or trunk-tissue types in the surrounding germ layers; we still maintain that head and trunk formation require qualitatively distinct factors (i.e. triple inhibition of WNT, BMP and Nodal signaling for head development vs BMP inhibition plus active Nodal and Wnt signaling for trunk development). Rather, here we focused on the organizer's own architecture as key to understand how these different instructions are handed-out in quantitative, spatial and temporal coordination.

Specifically, we found that the head-organizer - here defined as the anterior endoderm expressing the head inducers *Cerberus* - is established by the activities of two opposing signaling centers: one is the trunk organizer, emanating Nodal that induces *Cerberus* in the abutting endoderm, and a second center located in the deep, anterior-most endoderm defined by ADMP signaling that opposes their expression. ADMP is also produced in the trunk organizer as an effect of Nodal induction (Martello et al., 2007), but is not allowed to signal close to its production area (discussed below). These signaling centers are not simply fighting each other but, crucially, they reciprocally adjust their strength and range of activity: fluctuations in Nodal signaling will be rebalanced by coherent variations in ADMP signaling and viceversa (Figure 16A). This mechanism ensures that expression of the head inducers in the anterior endoderm is kept proportional to signals generated in the trunk organizer and buffered against their fluctuations.

**New functions for Nodal and Nodal-antagonists within the Organizer.**

For ectoderm cells responding to organizer signals, Nodal attenuation is critical to prevent the spreading of the trunk territory in the anterior part of the embryo so that the head can develop (Niehrs, 2004; Piccolo et al., 1999). This is mediated by the anti-Nodal functions of Cerberus and Lefty emanating from the organizer and by factors in the responding tissues, such as the Smad4 inhibitor Ectodermin and the multivalent antagonist Coco(Bell et al., 2003; Dupont et al., 2009; Dupont et al., 2005). This redundancy perhaps explains why the fraction of mice double knock-out for *Cerberus* and *Lefty-1* passing gastrulation does not show head defects and even displays rostral duplications in secondary axes (Perea-Gomez et al., 2002).

Beyond these roles in tissues outside of the organizers, this work also sheds new light on the role of Nodal antagonism as an intimate patterning element of the organizer,

rather than as head-inducer *per se*. As Nodal levels increase, expression of *Cerberus* in anterior endoderm also raises; in part, this is a feedback to limit the potentially explosive Nodal auto-induction loop, but also serves as permissive element for ADMP signaling. The system self-regulates because ADMP, in turn, tends to quench back head-organizer gene expression, including *Cerberus* expression, re-establishing the equilibrium between Nodal and ADMP activity.

Notably, a critical element of the network is a TGFβ receptor, ACVR2a: this is shared between Nodal and ADMP but its post-transcriptional regulation by an abundant miRNA of the embryo, miR-15/16, imposes a burden on its expression (Martello et al., 2007). ACVR2a is thus available only in limited amount, such that the two ligands cannot signals simultaneously. In absence of Nodal antagonism, Nodal/ACVR2a receptors complexes dominate over ADMP/ACVR2a complexes, impeding ADMP signaling. ADMP activity indeed poses a potential fatal threat for the organizer, inhibiting expression of Chordin, Cerberus and its own expression as well (Dosch and Niehrs, 2000; Reversade and De Robertis, 2005). In part, ADMP is regulated by binding to Chordin, that shuttles it away guaranteeing ADMP long-range diffusion (Ben-Zvi et al., 2008). Here we propose that by titration of ACVR2a receptors, Nodal itself directly contributes to bar ADMP activity in its production site. It is Cerberus itself - in concert with Lefty - that allows the competition between Nodal and ADMP: in the ensuing dynamic equilibrium, ADMP signaling is turned-on in the farthest anterior endoderm, while Nodal prevails in the posterior endoderm abutting the trunk organizer (i.e. close to its source) (Figure 16A). Thus, we propose that the function of Nodal antagonism within the organizer is ultimately anti-head, opposite to its pro-head function in the outside territories.

The vertebrate genome encodes many TGFβ-related ligands but much fewer type I and type II receptors and only handful of Smads; promiscuity in receptor usage has been hypothesized as a main determinant for context-dependent responses (Feng and Derynck, 2005). Moreover, a wealth of research indicates that Smads and Receptor can be limited in vivo by multiple mechanisms including miRNA regulation, sequestration, phosphorylation and ubiquitination (Itoh and ten Dijke, 2007). The present work at least suggests that ligand competition for shared receptors might serve as widespread tool for TGFβ antagonism. It will be therefore important to test if such remarkably simple

interplay may be at work in other contexts to regulate signal intensity, coordination and temporal/spatial signaling dynamics.

**miRNAs, signal transduction and biological robustness**

Our findings suggest the interesting notion that signaling pathways may represent ideal candidates for miRNA regulation, in virtue of the sharp dose-sensitive nature of their effects and extensive usage of feedforward and feedback loops for signaling cross-talk and tight control over gene expression. The dynamic kinetic properties of miRNAs are ideally suited to buffer fluctuation in gene networks: miRNA processing is faster than protein translation, allowing miRNAs to affect gene expression with shorter delay than transcription factors and thus endowing cells with exquisite temporal and quantitative precision over cell signaling (Hornstein and Shomron, 2006; Li et al., 2009; Tsang et al., 2007). This work provides experimental evidence for these theories.

At the same time, it did not escape to us that the phenotypic consequences of miR-15/16 were, *per se*, modest until we challenged our experimental system with perturbations, such as partial knockdown of β-catenin; in hindsight, it is noteworthy that only then an unexpected complexity of new gene interactions in Spemann's organizer biology could be revealed. If miRNAs are in general part of robustness loops, this points to the new challenge of designing more sophisticated experimental assays as proxy of the cell's complexity and interactions within tissues.

It will be interesting to verify if the logic of cell-cell interactions here described applies in other tissues to quantitatively regulate complex cell behaviors in response to TGFβ or other growth factors. Conversely, the assembly of such intriguing set of circuits into a more complex and self-organizing program may guide applications in tissue regenerations or help "synthetic biology" efforts for bottom-up studies of natural system and engineering applications.

## MATERIALS AND METHODS

### Manipulation of Xenopus embryos and In Situ Hybridization

***Embryo Collection*** Xenopus Laevis frogs have been kept in tanks at 18° C in an animal room. Females frogs were injected with 50 U of Follicle-stimulating hormone (FSH) to induce ovulation a week before the experiment, and the night before with 800 U of Human chorionic gonadotropin (HCG).

The morning after eggs were artificially fertilized with a piece of testicle excised from a male frog and kept in ice. After 2 minutes we left fertilized eggs in water for 15 minutes and then 15 minutes in Barth 0.1X solution (Piccolo et al., 1996). Embryos were then treated with L-cystein 3% solution for 8 minutes to eliminate the gelly coat. Embryos were then transferred in Barth 0.1X solution at room temperature after the first division and then selected and transferred in Barth 1X solution.

Embryos were injected at 2-4 cells stage with mRNA synthetized in vitro. After 20 minutes of recovery from injection, embryos were transferred in Barth 0.1X solution and left to develop until the desired stage.

***Fixation***. Selected embryos were transferred to a 5 ml screw cap glass vial filled with distilled water. After the embryos settled, the water was removed and the vials were filled to the brim with MEMFA (0.1M Mops pH7.4, 2mM EGTA, IITIM MgSO4, 3.7% formaldehyde). Embryos were allowed to fix at room temperature for 1.5 to 2h on a Labquake rotator (Labindustries, Inc). MEMFA was made freshly from a stock of 10x salts and 37% formaldehyde. The fix was removed and replaced with methanol. After a few minutes of equilibration with the methanol, the embryos were stored at —20°C.

***Probes***. The linearized DNA templates for the probes used in this study were used for *in vitro* transcription reactions in the presence of digoxigenin- 11-UTP with either T3, T7 or SP6 RNA polymerase. Probe purification was as described by http://www.hhmi.ucla.edu/derobertis/).

***In situ hybridization*** Fixed embryos in methanol were gradually rehydrated with ME (90% methanol, 10% 0.5 M EGTA) and PTw (lX PBS+0.1% Tween-20) by 5 min incubations in ME, 75% ME+25 % PTw, 50 % ME+50 % PTw, 25 % ME+75 % PTw, 100% PTw. They were then washed three times, 5 min each, in PTw. vials were filled almost completely with liquid and rocked on a nutator. The embryos were then incubated at room temperature in proteinase K (in PTw) for 15 min. At the end of the proteinase K treatment, embryos were washed twice, 5 min each, in PTw and were

refixed for 20 min with 4% paraformaldehyde in lxPBS at room temperature. Paraformaldehyde yielded marginally better results than formaldehyde. The refix was followed by five washes, 5 min each in PTw. Since the embryos are somewhat delicate after protease treatment, the rocking steps are done by laying the vials horizontally on the nutator and filling the vials to reduce turbulence.

Hybridization buffer (1 ml) was added to a near empty tube and the embryos allowed to settle and equilibrate for a few minutes. The hybridization buffer was changed and the embryos were prehybridized for 1h at 50°C. The prehybridization buffer was replaced with fresh hybridization solution containing the probe (5-10 μg/ml) and embryos were incubated overnight at 65°C. At the end of the hybridization the probe was saved. We find that the probe can be recycled up to 3 times. The embryos were brought from hybridization buffer to 2X SSC gradually by 1.5 ml changes of the following solutions: 75% hyb+25% 2X SSC, 50% hyb+50% 2X SSC and 25% hyb+75 % 2X SSC each wash for 10min at 37°C in a shaking waterbath. This was followed by two washes 20 min in 2X SSC at 37°C. From 2xSSC the embryos were transferred to 0.2X SSC and washed twice in 0.2X SSC for 30min, at 55°C; and stepped back to PTw, 5-10min changes of 75% 0.2X SSC+25% PTw, 50% 0.2X SSC+50% PTw, 25% 0.2X SSC+75% PTw and 100% PTw.

***Detection***. RNA hybrids were detected by immunohistochemistry. The PTw was removed and replaced with PTw+10% heat-inactivated goat serum (Gibco; the serum is heated at 56°C for 30min). This step saturates non-specific immunoglobulin- binding sites. Vials were rocked vertically at room temperature for lh. This solution was replaced with PTw+10 % goat serum containing a 1/1000 dilution of the affinity-purified sheep anti-digoxigenin coupled to alkaline phosphatase antibody. Tubes were rocked vertically overnight at 4°C. To remove excess antibody, the embryos were washed at least 3 times 1 h each with PBT at room temperature (filled up vials and horizontal rocking). For the chromogenic reaction with alkaline phosphatase, embryos were washed 3 times, 5 min each at room temperature with l00mM Tris pH9.5, 50mM MgCl2. 100mM NaCl, 0.1 % Tween 20 and 1 mM Levamisol added freshly to inhibit endogenous alkaline phosphatase. The last wash was replaced with BM Purple. Embryos were stained at 4°C for 24-48 hours solution until the desired staining was reached and then fixed in MEMFA overnight.

**Microinjection of Xenopus embryos: gain- and loss-of-function assays.**

RNA was synthesized using Message Machine kit (Ambion) from expression vectors (pCS2-ADMP; pCS2-CerS; pCS2-Xnr1(Nodal); pCS2-ACVR2a), linearized with NotI and transcribed with SP6 RNA polymerase as described previously (Piccolo et al., 1996).

Mature miR-15 sequences were:

wt-sense 5'UAG CAG CAC AUA AUG GUU UGU GUU3';

wt-antisense 5'CAC AAACCA UUA UGU GCU GGA UUU3';

mut-sense 5'UUC GUC AAC AUA AUG GUUUGU GUU3';

mut-antisense 5'CAC AAA CCA UUA UGU UGA CCU UUU3'

(Invitrogen).

AntimiR reagents were puchased from Dharmacon or Ambion (antimiR-15: 5'-AAU CCA CAA ACC AUU AUG UGC UGC UAC UUU-3'; antimiR-16: 5'-AAU CCU CCAGUA UUU ACG UGC UGC UAA GGC -3'). In the course of this study, we switched from anti-miR to Morpholinos oligonucleotides (MO) because of reduced toxicity of the latter reagent. MO targeting miR-15 and miR-16 were generated from the same sequences used in anti-miR by GeneTools Inc.

Antisense MO for *Xenopus laevis* Admp, beta-catenin, Cerberus, Lefty consisted of the following sequences: Admp MO, 5′-GGTCCATCTCATCAAGCTGCAGCTC-3′; Beta-catenin MO, 5′-TTT CAA CCG TTT CCA AAG AAC CAG G-3′); *Cer*-MO (5′-ACT TGC TGT TCC TGC ACT GTG C-3′); Lefty-MO 5'-AAAGATTTGGTAGTGACACCCATTC-3 and control-MO (5′-CCT CTT ACC TCA GTT ACA ATT TAT A-3′)

MOs were resuspended in sterile water to a concentration of 1 mM, which was then further diluted to give a working solution of 0.25 mM (doses are indicated in the Figure Legends). Prior to microinjections, MO mixtures were heated at 95°C for 25 sec. and placed on ice. When multiple MOs were tested, a mixture was prepared and embryos were injected four times radially at the two- to four-cell stage. A total of 8 nl (two times 4 nl or four times 2 nl) morpholino solutions were injected at the 2-cell stage or 4 nl (two times 2 nl) of morpholino solution injected at the 8-cell stage.

For mRNA microinjections, embryos were microinjected four times in each blastomere at the four-cell stage) with the mRNA doses indicated in Figure Legend (i.e. for 100 pg

of *Admp* mRNA = 25 pg were injected four times, in each blastomere at the four-cell stage). Embryos were collected at the indicated stages and processed for in situ hybridization or photographed for whole embryo phenotypes.

For **luciferase assays,** embryos were radially injected with 40 pg of reporter plasmid Mix.2 or ID1BRE (BMP-Responsive-Element from the Vent.2 promoter, a BMP target gene) plus 150 pg of *lacZ* mRNA and collected at early gastrula. Luciferase values were normalized to beta-gal activity that, typically, did not oscillate more that 25% within the same batch. For each experiment, the normalized luciferase value is the mean of at least three independent embryos' sets, each containing 5 embryos.

Luciferase was measured using the Luciferase Assay System (Promega)

**Embryological methods**

For grafts shown in Figure 15, Blastula-stage embryos (stage 9) were manually dechorionated in 0.3X modified Barth's solution, bisected into two equal halves across the prospective dorsoventral axis using a surgical blade or sharp forceps. From the dorsal halves, the leading edge anterior endoderm was identified by the Brachet's cleft and explanted from surrounding deep endoderm, mesoderm and ectoderm. Explants were cultured in fresh 0.3X Barth's solution (Piccolo et al., 1996) before being transplanted into a host embryo by introduction into the blastocelic cavity.

**Cell cultures and transfections.**

Cell lines HEK293T (Human embryonic kidney) and HepG2 (Human hepatoma) were purchased from ATCC. HEK293T were cultivated in DMEM, 10% serum, 20mM L-Glutamin, 1X Penicillin/Streptomicin. HepG2 were cultivated in DMEM supplemented with 10% serum, 40mM L-Glutamin, 1X Penicillin/Streptomicin, 1X non essential aminoacids. 293T cells were transfected with calcium phosphate (Piccolo et al., 1996), and HepG2 with Lipofectamine2000 (Invitrogen) (Dupont et al., 2009). Plasmid DNA (300ng/cm$^2$) was concentrated and precipitated with sodium acetate an ethanol and suspended in sterile water before mixing with transfection reagents. For transcriptional response assays, LacZ constitutive expression vector (150 ng) was always co-transfected to normalize for transfection efficiency using a colorimetric reaction using

CPRG (as described in Dupont et al., 2009). pCS2-ACVR2a was cotransfected at 500ng/cm$^2$.

For ACVR2a siRNA knockdown, HepG2 were transfected one day in advance plasmid transfection with dsRNA oligos (Ambion, 75 ng/cm$^2$). For this, cells were transfected using the RNAiMax transfection reagent (Invitrogen). ACVR2a siRNA sequences were as described (Martello et al., 2007). Mature miRNA (75 ng/ cm$^2$) were transfected with RNAiMax. Each transfection was carried out at least twice independently, each in triplicate. Luciferase was measured using the Luciferase Assay System (Promega)

**Antibodies, co-immunoprecipitations and Western Blotting**

Anti-His and anti-Myc antobodies were purchased by Santa-Cruz and Covance, respectively. Xenopus embryos or cultured mammalian cells were harvested by sonication in Ub-lysis buffer (Dupont et al., 2009)(25µl/cm$^2$). Proteins were loaded according to Bradford quantitation, run in commercial 4-12% or 10% Nupage MOPS acrylamide gels (Invitrogen) and transferred onto PVDF membranes (Immobilon-P) by wet electrophoretic transfer. In general, blots were blocked one hour at room temperature with 0,5% non-fat dry milk (BioRad) in PBSw (0,05% Tween) and incubated overnight at 4°C with primary antibodies. Secondary antibodies were incubated 50min. at room temperature. Washes after antibody incubations were done on an orbital shaker, three times 10 min, with 1X PBS 0,05% Tween-20. Blots were developed with Pico or Dura SuperSignal West chemiluminescent reagents (Pierce).

For coimmunoprecipitation experiments and receptor binding assay shown in Figure 11, ADMP protein was produced in the conditioned media of 293T cells transfected with pCS2-ADMP-Myc (Piccolo et al., 1996). Protein A beads (Pierce) were bound to human recombinant chimeric ALK-2-Fc, ACVR2a-Fc, BMPR-II-Fc (from R&D Systems Inc) in PBS+BSA 0.1%+0.3% NP40 for one hour. 1/10 of ADMP containing media was added as indicated in Figure 11A and incubated 4 hours at 4°C. After 3 washes (20min. in total), beads were boiled in sample buffer (Tris pH 6.8, 2% SDS, 0.1% Blue Bromophenol, 10% Glycerol).

**Immunohistochemistry**

Embryos (stage 10) were manually dechorionated in 0.3X modified Barth's solution, bisected into two equal halves (emisections) along the prospective dorsoventral axis using a surgical blade or sharp forceps. Explants were fixed overnight in PBS containing 10% paraformaldehyde and embedded in paraffin. Sections (10µm) were incubated with anti-pSmad1 antibody (1:200 dilution, Uppstate) and then developed with Vectastain ABC kit (Vector) according to the manufacturer's instructions.

# REFERENCES


Alon, U. (2007). Network motifs: theory and experimental approaches. Nat Rev Genet *8*, 450-461.

Barkai, N., and Ben-Zvi, D. (2009). 'Big frog, small frog'--maintaining proportions in embryonic development: delivered on 2 July 2008 at the 33rd FEBS Congress in Athens, Greece. Febs J *276*, 1196-1207.

Bartel, D.P. (2009). MicroRNAs: target recognition and regulatory functions. Cell *136*, 215-233.

Bartel, D.P., and Chen, C.Z. (2004). Micromanagers of gene expression: the potentially widespread influence of metazoan microRNAs. Nat Rev Genet *5*, 396-400.

Bell, E., Munoz-Sanjuan, I., Altmann, C.R., Vonica, A., and Brivanlou, A.H. (2003). Cell fate specification and competence by Coco, a maternal BMP, TGFbeta and Wnt inhibitor. Development *130*, 1381-1389.

Ben-Zvi, D., Shilo, B.Z., Fainsod, A., and Barkai, N. (2008). Scaling of the BMP activation gradient in Xenopus embryos. Nature *453*, 1205-1211.

Bouwmeester, T., Kim, S., Sasai, Y., Lu, B., and De Robertis, E.M. (1996). Cerberus is a head-inducing secreted factor expressed in the anterior endoderm of Spemann's organizer. Nature *382*, 595-601.

Brodersen, P., and Voinnet, O. (2009). Revisiting the principles of microRNA target recognition and mode of action. Nat Rev Mol Cell Biol *10*, 141-148.

Carthew, R.W., and Sontheimer, E.J. (2009). Origins and Mechanisms of miRNAs and siRNAs. Cell *136*, 642-655.

De Robertis, E.M. (2006). Spemann's organizer and self-regulation in amphibian embryos. Nat Rev Mol Cell Biol *7*, 296-302.

De Robertis, E.M., Larrain, J., Oelgeschlager, M., and Wessely, O. (2000). The establishment of Spemann's organizer and patterning of the vertebrate embryo. Nat Rev Genet *1*, 171-181.

Dosch, R., and Niehrs, C. (2000). Requirement for anti-dorsalizing morphogenetic protein in organizer patterning. Mech Dev *90*, 195-203.

Dupont, S., Mamidi, A., Cordenonsi, M., Montagner, M., Zacchigna, L., Adorno, M., Martello, G., Stinchfield, M.J., Soligo, S., Morsut, L.*, et al.* (2009). FAM/USP9x, a deubiquitinating enzyme essential for TGFbeta signaling, controls Smad4 monoubiquitination. Cell *136*, 123-135.

Dupont, S., Zacchigna, L., Cordenonsi, M., Soligo, S., Adorno, M., Rugge, M., and Piccolo, S. (2005). Germ-layer specification and control of cell growth by Ectodermin, a Smad4 ubiquitin ligase. Cell *121*, 87-99.

Farh, K.K., Grimson, A., Jan, C., Lewis, B.P., Johnston, W.K., Lim, L.P., Burge, C.B., and Bartel, D.P. (2005). The widespread impact of mammalian MicroRNAs on mRNA repression and evolution. Science *310*, 1817-1821.

Feng, X.H., and Derynck, R. (2005). Specificity and versatility in tgf-beta signaling through Smads. Annu Rev Cell Dev Biol *21*, 659-693.

Glinka, A., Wu, W., Delius, H., Monaghan, A.P., Blumenstock, C., and Niehrs, C. (1998). Dickkopf-1 is a member of a new family of secreted proteins and functions in head induction. Nature *391*, 357-362.

Glinka, A., Wu, W., Onichtchouk, D., Blumenstock, C., and Niehrs, C. (1997). Head induction by simultaneous repression of Bmp and Wnt signalling in Xenopus. Nature *389*, 517-519.

Harland, R., and Gerhart, J. (1997). Formation and function of Spemann's organizer. Annu Rev Cell Dev Biol *13*, 611-667.

Hornstein, E., and Shomron, N. (2006). Canalization of development by microRNAs. Nat Genet *38 Suppl*, S20-24.

Inomata, H., Haraguchi, T., and Sasai, Y. (2008). Robust stability of the embryonic axial pattern requires a secreted scaffold for chordin degradation. Cell *134*, 854-865.

Itoh, S., and ten Dijke, P. (2007). Negative regulation of TGF-beta receptor/Smad signal transduction. Curr Opin Cell Biol *19*, 176-184.

Jones, C.M., Kuehn, M.R., Hogan, B.L., Smith, J.C., and Wright, C.V. (1995). Nodal-related signals induce axial mesoderm and dorsalize mesoderm during gastrulation. Development *121*, 3651-3662.

Khokha, M.K., Yeh, J., Grammer, T.C., and Harland, R.M. (2005). Depletion of three BMP antagonists from Spemann's organizer leads to a catastrophic loss of dorsal structures. Dev Cell *8*, 401-411.

Li, X., Cassidy, J.J., Reinke, C.A., Fischboeck, S., and Carthew, R.W. (2009). A microRNA imparts robustness against environmental fluctuation during development. Cell *137*, 273-282.

Martello, G., Zacchigna, L., Inui, M., Montagner, M., Adorno, M., Mamidi, A., Morsut, L., Soligo, S., Tran, U., Dupont, S.*, et al.* (2007). MicroRNA control of Nodal signalling. Nature *449*, 183-188.

Martinez, N.J., Ow, M.C., Barrasa, M.I., Hammell, M., Sequerra, R., Doucette-Stamm, L., Roth, F.P., Ambros, V.R., and Walhout, A.J. (2008). A C. elegans genome-scale microRNA network contains composite feedback motifs with high flux capacity. Genes Dev *22*, 2535-2549.

Meno, C., Gritsman, K., Ohishi, S., Ohfuji, Y., Heckscher, E., Mochida, K., Shimono, A., Kondoh, H., Talbot, W.S., Robertson, E.J.*, et al.* (1999). Mouse Lefty2 and zebrafish antivin are feedback inhibitors of nodal signaling during vertebrate gastrulation. Mol Cell *4*, 287-298.

Milo, R., Shen-Orr, S., Itzkovitz, S., Kashtan, N., Chklovskii, D., and Alon, U. (2002). Network motifs: simple building blocks of complex networks. Science *298*, 824-827.

Moos, M., Jr., Wang, S., and Krinks, M. (1995). Anti-dorsalizing morphogenetic protein is a novel TGF-beta homolog expressed in the Spemann organizer. Development *121*, 4293-4301.

Murchison, E.P., Partridge, J.F., Tam, O.H., Cheloufi, S., and Hannon, G.J. (2005). Characterization of Dicer-deficient murine embryonic stem cells. Proc Natl Acad Sci U S A *102*, 12135-12140.

Niehrs, C. (2004). Regionally specific induction by the Spemann-Mangold organizer. Nat Rev Genet *5*, 425-434.

Norris, D.P., Brennan, J., Bikoff, E.K., and Robertson, E.J. (2002). The Foxh1-dependent autoregulatory enhancer controls the level of Nodal signals in the mouse embryo. Development *129*, 3455-3468.

Osada, S.I., Saijoh, Y., Frisch, A., Yeo, C.Y., Adachi, H., Watanabe, M., Whitman, M., Hamada, H., and Wright, C.V. (2000). Activin/nodal responsiveness and asymmetric expression of a Xenopus nodal-related gene converge on a FAST-regulated module in intron 1. Development *127*, 2503-2514.

Perea-Gomez, A., Vella, F.D., Shawlot, W., Oulad-Abdelghani, M., Chazaud, C., Meno, C., Pfister, V., Chen, L., Robertson, E., Hamada, H.*, et al.* (2002). Nodal antagonists in the anterior visceral endoderm prevent the formation of multiple primitive streaks. Dev Cell *3*, 745-756.

Piccolo, S., Agius, E., Leyns, L., Bhattacharyya, S., Grunz, H., Bouwmeester, T., and De Robertis, E.M. (1999). The head inducer Cerberus is a multifunctional antagonist of Nodal, BMP and Wnt signals. Nature *397*, 707-710.

Piccolo, S., Sasai, Y., Lu, B., and De Robertis, E.M. (1996). Dorsoventral patterning in Xenopus: inhibition of ventral signals by direct binding of chordin to BMP-4. Cell *86*, 589-598.

Plouhinec, J.L., and De Robertis, E.M. (2007). Systems biology of embryonic morphogens. Mol Biosyst *3*, 454-457.

Reversade, B., and De Robertis, E.M. (2005). Regulation of ADMP and BMP2/4/7 at opposite embryonic poles generates a self-regulating morphogenetic field. Cell *123*, 1147-1160.

Schneider, V.A., and Mercola, M. (1999). Spatially distinct head and heart inducers within the Xenopus organizer region. Curr Biol *9*, 800-809.

Shen-Orr, S.S., Milo, R., Mangan, S., and Alon, U. (2002). Network motifs in the transcriptional regulation network of Escherichia coli. Nat Genet *31*, 64-68.

Spemann, H., and Mangold, H. (2001). Induction of embryonic primordia by implantation of organizers from a different species. 1924. Int J Dev Biol *45*, 13-38.

Stark, A., Brennecke, J., Bushati, N., Russell, R.B., and Cohen, S.M. (2005). Animal MicroRNAs confer robustness to gene expression and have a significant impact on 3'UTR evolution. Cell *123*, 1133-1146.

Takahashi, S., Yokota, C., Takano, K., Tanegashima, K., Onuma, Y., Goto, J., and Asashima, M. (2000). Two novel nodal-related genes initiate early inductive events in Xenopus Nieuwkoop center. Development *127*, 5319-5329.

Tam, P.P., and Loebel, D.A. (2007). Gene function in mouse embryogenesis: get set for gastrulation. Nat Rev Genet *8*, 368-381.

Tam, P.P., and Steiner, K.A. (1999). Anterior patterning by synergistic activity of the early gastrula organizer and the anterior germ layer tissues of the mouse embryo. Development *126*, 5171-5179.

Tang, F., Kaneda, M., O'Carroll, D., Hajkova, P., Barton, S.C., Sun, Y.A., Lee, C., Tarakhovsky, A., Lao, K., and Surani, M.A. (2007). Maternal microRNAs are essential for mouse zygotic development. Genes Dev *21*, 644-648.

Tsang, J., Zhu, J., and van Oudenaarden, A. (2007). MicroRNA-mediated feedback and feedforward loops are recurrent network motifs in mammals. Mol Cell *26*, 753-767.

Vodicka, M.A., and Gerhart, J.C. (1995). Blastomere derivation and domains of gene expression in the Spemann Organizer of Xenopus laevis. Development *121*, 3505-3518.

Yi, R., Poy, M.N., Stoffel, M., and Fuchs, E. (2008). A skin microRNA promotes differentiation by repressing 'stemness'. Nature *452*, 225-229.

Zimmerman, L.B., De Jesus-Escobar, J.M., and Harland, R.M. (1996). The Spemann organizer signal noggin binds and inactivates bone morphogenetic protein 4. Cell *86*, 599-606.

# FIGURE LEGEND

***Figure 1. The anatomy of Xenopus development.***

**A.** The egg is radially symmetrical and divided into an animal and a vegetal domain.

**B.**One hour after fertilization, an unpigmented dorsal crescent is formed in the fertilized egg opposite the sperm entry point.

**C.** *Blastula stage* (9 h of development). At this stage the three germ layers become defined: ectoderm, mesoderm and endoderm.

**D.** *Gastrula stage* (10 h). The morphogenetic movements of gastrulation lead to the formation of the vertebrate body plan, patterning the ectoderm, mesoderm and endoderm.

**E.** Neurula stage (14 h), the neural plate, or future central nervous system (CNS), becomes visible in dorsal ectoderm.

**F.** Tail bud stage. The neuronal tube is located between the epidermis and the notochord. Blastopore gives rise to the anus, and the mouth is generated by secondary perforation.

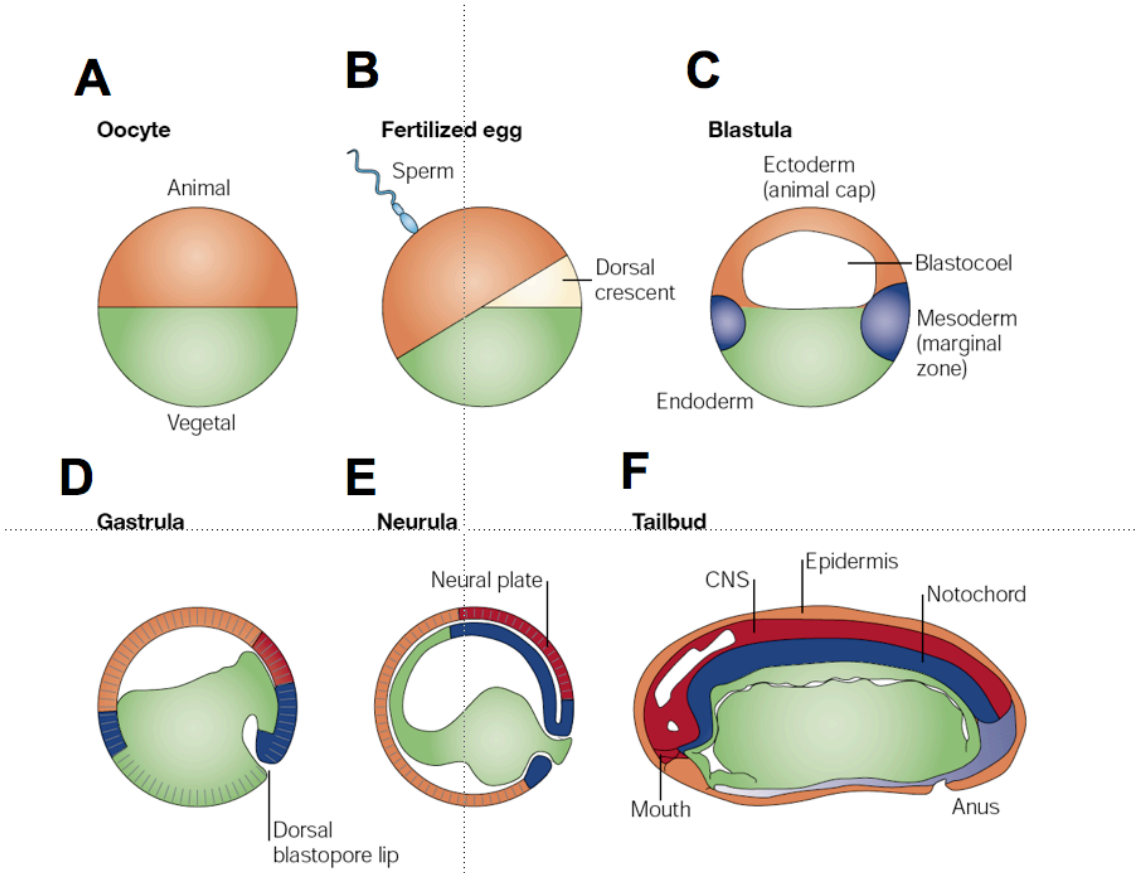
A
Oocyte
Animal
Vegetal
B
Fertilized egg
Sperm
Dorsal crescent
C
Blastula
Ectoderm (animal cap)
Blastocoel
Mesoderm (marginal zone)
Endoderm
D
Gastrula
Dorsal blastopore lip
E
Neurula
Neural plate
F
Tailbud
CNS
Epidermis
Notochord
Mouth
Anus

FIG.1

***Figure2. Dorsal determinants and the transport of membrane vesicles to the dorsal side.***

**A.** After fertilization, parallel arrays of microtubules extend from the centriole of the sperm, and transport small membrane vesicles from the vegetal towards the dorsal animal pole. The inset shows that the dorsal determinant vesicles are associated with Dishevelled (Dsh), a component of the Wnt signal transduction pathway. Kinesins are molecular motors that can transport vesicles towards the plus ends of microtubules. β-Catenin is found in a large cytoplasmic complex that includes Axin, APC (adenomatous polyposis coli) and GSK-3 (glycogen synthase kinase 3). GSK-3 negatively regulates β -Catenin through phosphorylations that target β-Catenin for degradation by the proteasome. On stimulation of the Wnt pathway, β-Catenin is stabilized on the dorsal side and can be found in the nucleus, where, together with TCF-3, it activates various target genes, including homeobox and Nodal-related genes (*Xnrs*).

**B.** Siamese embryo obtained after microinjection of Wnt, β-Catenin or other positive mediators of Wnt pathway.

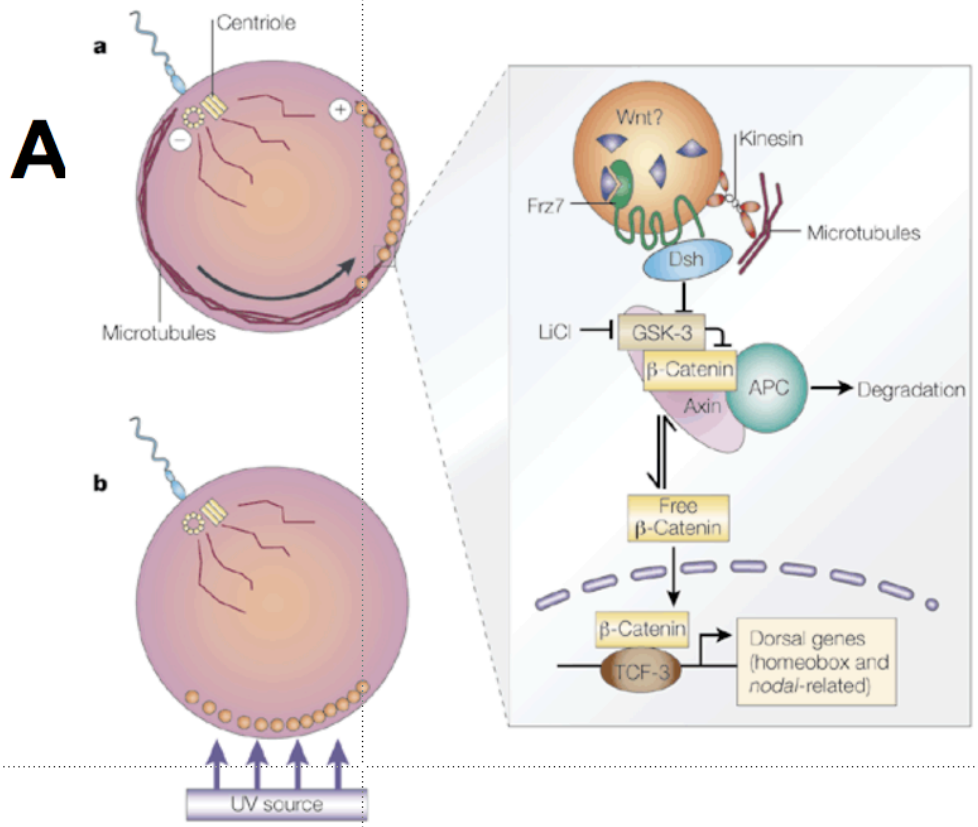
A
a
Centriole
Microtubules
b
UV source
Wnt?
Kinesin
Frz7
Microtubules
Dsh
LiCl
GSK-3
β-Catenin
APC
Degradation
Axin
Free
β-Catenin
β-Catenin
TCF-3
Dorsal genes
(homeobox and
nodal-related)


B

FIG.2

***Figure3. Formation of Nodal gradient in the endoderm.***

During cortical rotation, β-Catenin becomes enriched at the dorsal side of the embryo, as detailed in Figure 2. The asymmetrical distribution of β-Catenin leds to asymmetry in Nodal activity. Nodal is a TGFβ family member, signaling via Smad2/3. Nodal activity is a gradient along the dorso-ventral axis. This gradient has its peak on the dorsal side, essential for induction and patterning of the Spemann organizer.

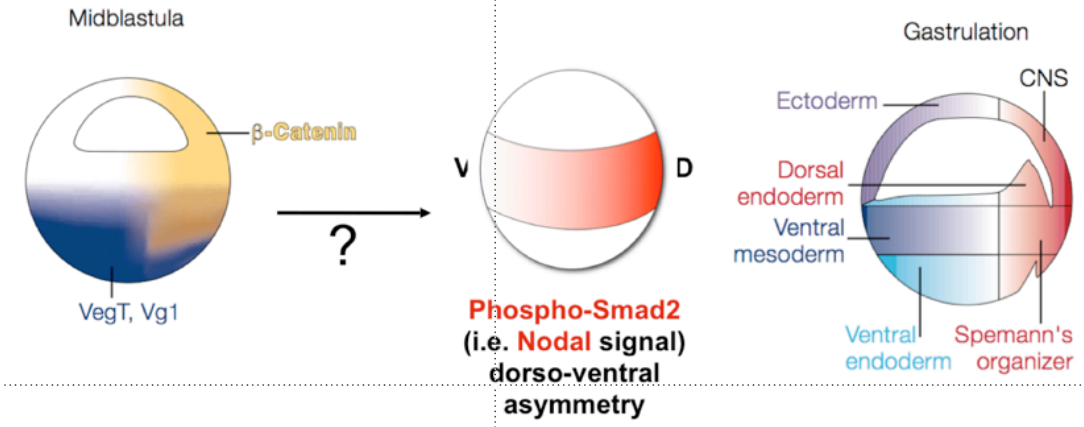
Midblastula
β-Catenin
VegT, Vg1
?
V
D
Phospho-Smad2
(i.e. Nodal signal)
dorso-ventral
asymmetry
Gastrulation
CNS
Ectoderm
Dorsal
endoderm
Ventral
mesoderm
Ventral
endoderm
Spemann's
organizer

**FIG.3**

***Figure 4. Transforming Growth Factor-β(TGFβ).***

On the cell surface TGFβ ligands bind to the serin/treonin kinase receptor (receptors type I and II). The interaction between the receptors causes activation by phosphorylation of the Smad receptors (R-Smand), intracellular signaling transducers. R-Smads now are able to bind to Smad4 (co-Smad) and to get into the nucleus. Inside the nucleus they control the expression of specific target genes.

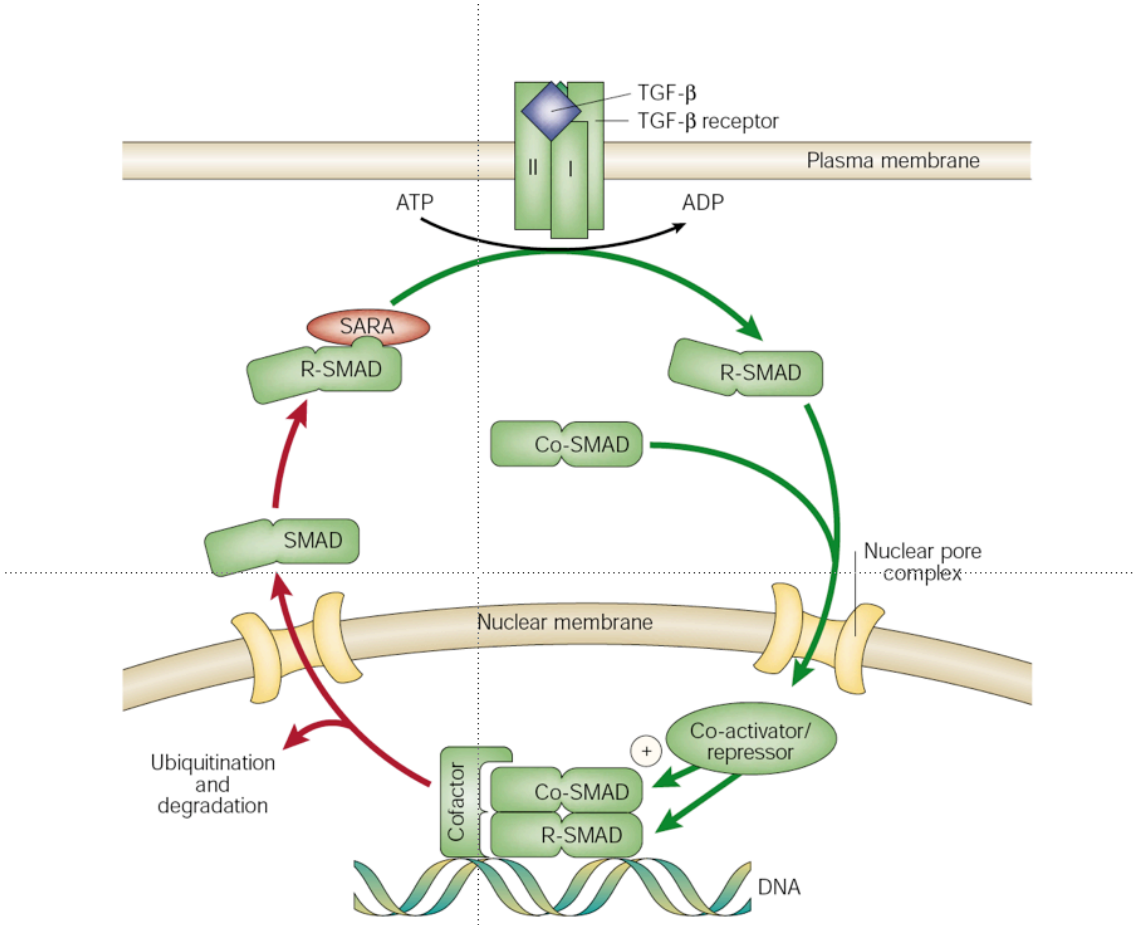
TGF-β
TGF-β receptor
II
I
Plasma membrane
ATP
ADP
SARA
R-SMAD
R-SMAD
Co-SMAD
SMAD
Nuclear pore complex
Nuclear membrane
Co-activator/ repressor
+
Ubiquitination and degradation
Cofactor
Co-SMAD
R-SMAD
DNA

FIG.4

***Figure 5. The Spemann Organizer graft.***

**A.** The dorsal blastopore lip of Xenopus embryo (early gastrula stage) is grafted in an ectopic location of a host embryo (same stage). This tissue is able to recruit neighboring cells to start gastrulation movements and to form a secondary axis.

**B.** Siamese embryos generated after transplantation of the Spemann Organizer (picture taken from De Robertis and Kuroda, 2004).

A

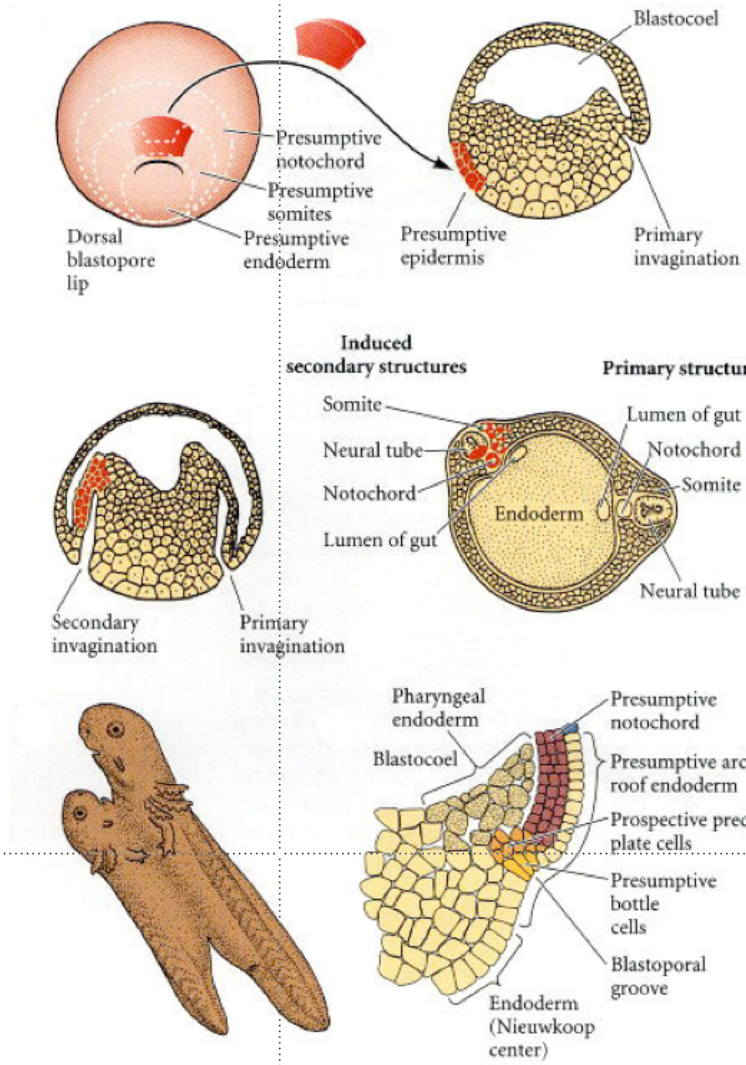
Blastocoel
Presumptive notochord
Presumptive somites
Presumptive endoderm
Dorsal blastopore lip
Presumptive epidermis
Primary invagination
Induced secondary structures
Primary structures
Somite
Neural tube
Notochord
Lumen of gut
Endoderm
Lumen of gut
Notochord
Somite
Neural tube
Secondary invagination
Primary invagination
Pharyngeal endoderm
Blastocoel
Presumptive notochord
Presumptive archenteron roof endoderm
Prospective prechordal plate cells
Presumptive bottle cells
Blastoporal groove
Endoderm (Nieuwkoop center)

B

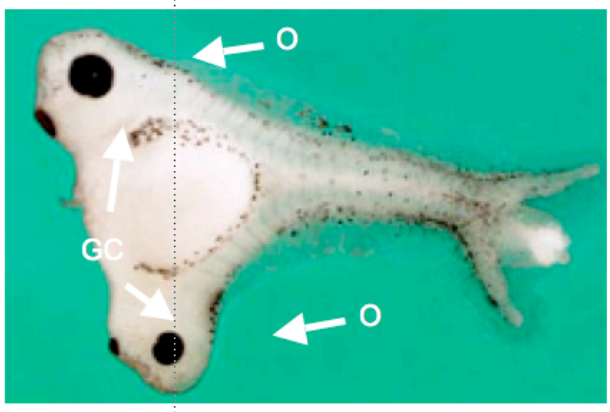
O
GC
O

FIG.5

***Figure 6. The Organizer "inducers" are growth factors antagonists.***

**A.**Table recapitulating the main head and trunk inducers. These extracellular proteins are all antagonists of growth factors.

**B.** Scheme of the head organizer region (endomesoderm), orange circle, and the presumptive trunk organizer, circled in blue, at stage 10,5 (early gastrula) and stage 11 (middle gastrula).

**C.** In situ hybridization of Xenopus embryos at stage 10,5 and stage 11 using Cerberus as a marker for the head organizer and Chordin as a marker for the trunk organizer.

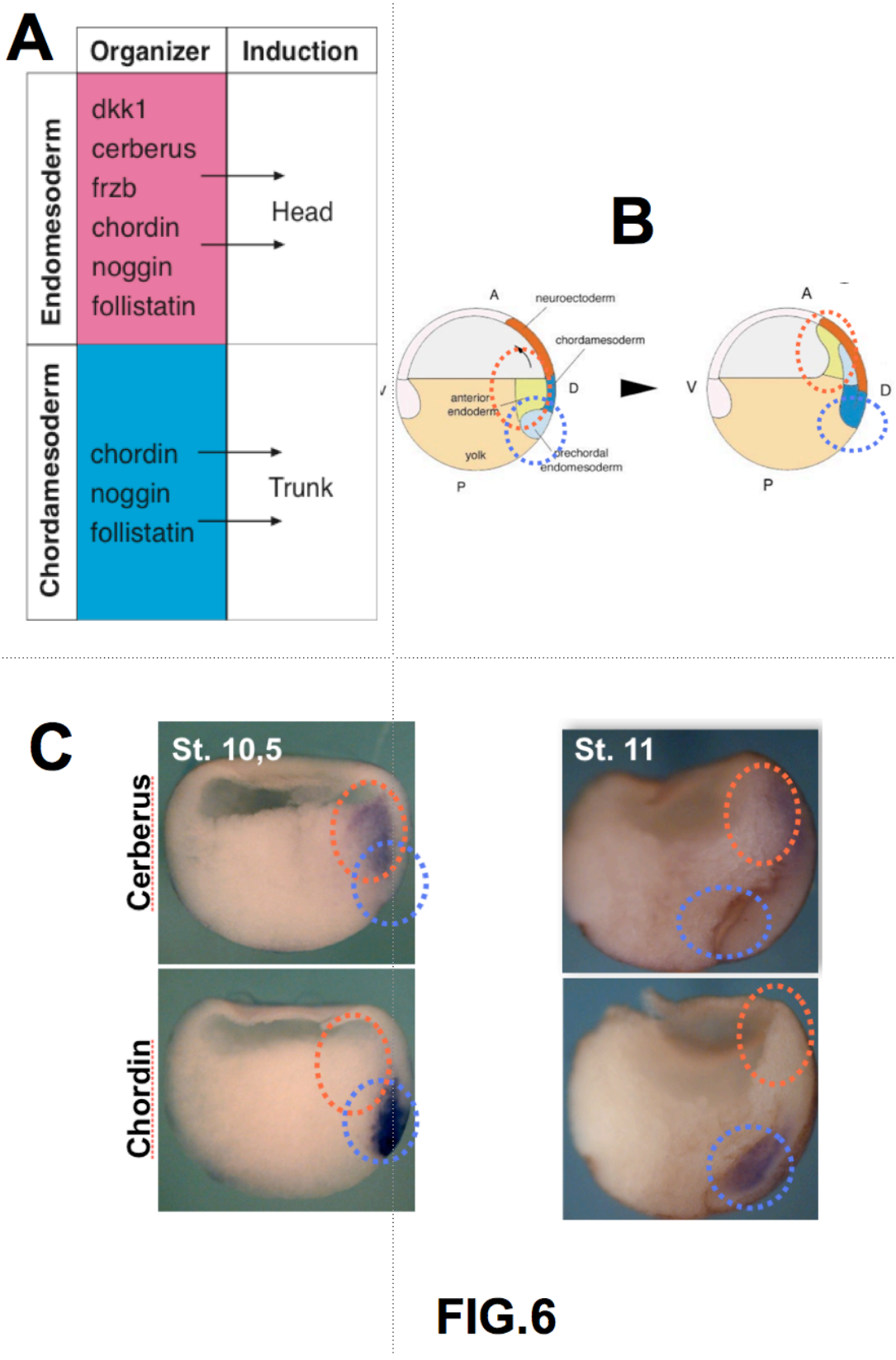
A
Organizer
Induction
Endomesoderm
dkk1
cerberus
frzb
chordin
noggin
follistatin
Head
Chordamesoderm
chordin
noggin
follistatin
Trunk
B
A
neuroectoderm
chordamesoderm
D
V
anterior endoderm
yolk
prechordal endomesoderm
P
A
V
D
P
C
Cerberus
St. 10,5
St. 11
Chordin

FIG.6

***Figure 7. Biogenesis of the microRNA.***

**A.** microRNA are first transcribed as part of longer precursors (pri-miRNA) (1), that fold on themselves to form hairpin structures. pri-miRNAs are then processed in the nucleus by the Drosha complex (2), transported into the cytoplasm via exportin 5 (3), where they undergo final processing by the Dicer ribonuclease (4). Mature miRNAs are rapidly unwounded to be incorporated in the RNA-induced silencing complex (RISC) by associating with Argonaute proteins (5). Within the RISC, the single-stranded miRNA guides target selection, causing inhibition of mRNA translation and/or stability (6).

**B.** miRNAs are ideally suited to participate in signaling loops. miRNAs in coherent feed-forward loops. In the absence of signal, the expression of a target (T) is kept repressed by a miRNA. Upon signaling (S), the target is activated directly but also through inhibition of the miRNA, resulting in coherent/coperative regulation. miRNAs in incoherent feed-forward loops: at difference with the previous example, in this case the signal (S) directly activates the target, but at the same time promotes its inhibition by the miRNA, resulting in two opposing regulations.

A

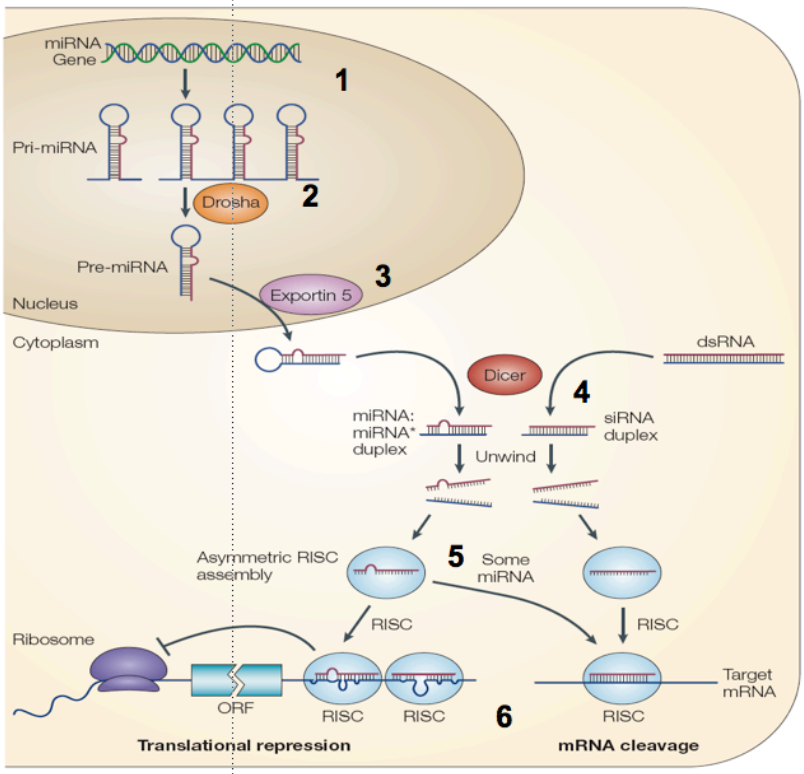
miRNA Gene
1
Pri-miRNA
Drosha
2
Pre-miRNA
3
Exportin 5
Nucleus
Cytoplasm
dsRNA
Dicer
4
miRNA: miRNA* duplex
siRNA duplex
Unwind
Asymmetric RISC assembly
5
Some miRNA
RISC
RISC
Ribosome
ORF
RISC
RISC
6
RISC
Target mRNA
Translational repression
mRNA cleavage

B

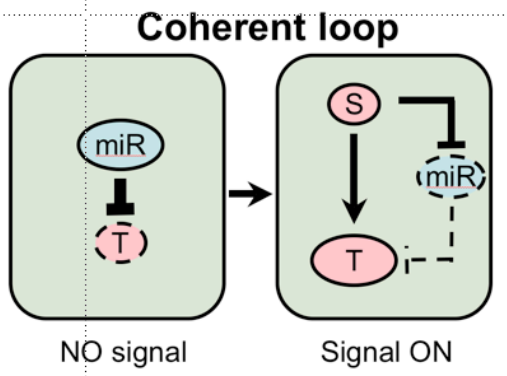
Coherent loop
miR
T
S
miR
T
NO signal
Signal ON

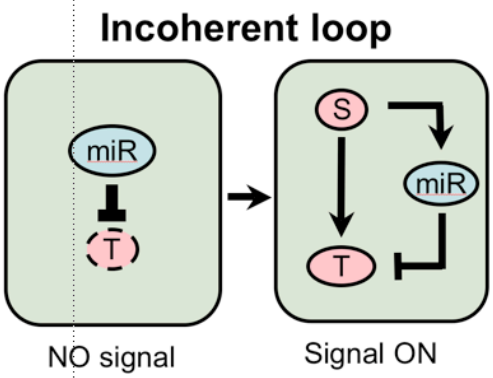
Incoherent loop
miR
T
S
miR
T
NO signal
Signal ON

FIG.7

***Figure 8. miR-15/16 confers robustness to head development by regulating ADMP/ACVR2a signaling***

**(A-H)** Embryos injected with Control morpholino (Control MO, 60ng) or with decreasing doses of β-catenin morpholino (β-cat MO, from 60ng/embryo - class I embryos - to 4ng/embryo - class III embryos) were harvested at stage 22 and stained by in situ hybridization for the head markers *Rx1* (eye field) and *XAG1* (cement gland) or for the pan-neural marker *Sox2*, staining both the head and trunk neural tissue.

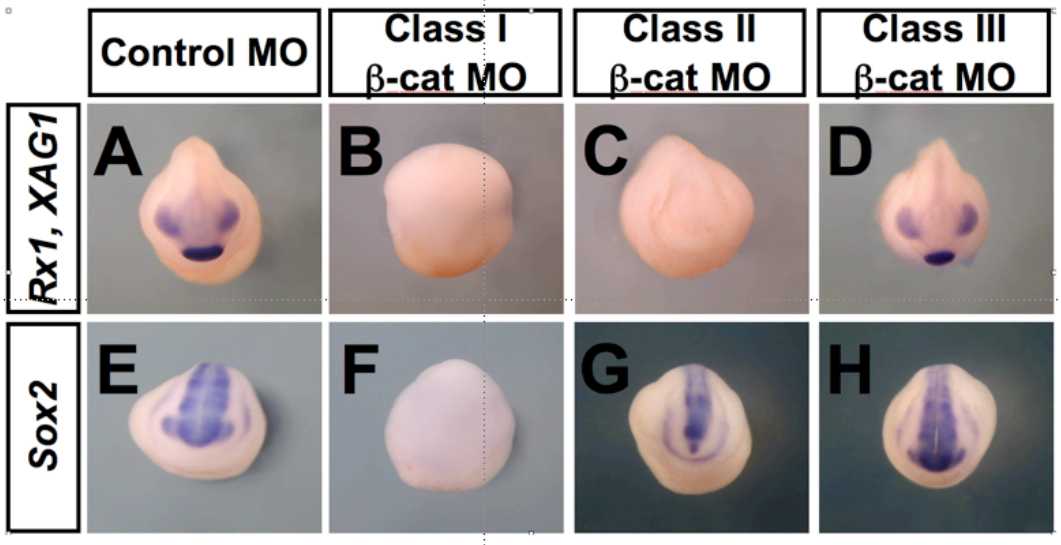
Control MO
Class I β-cat MO
Class II β-cat MO
Class III β-cat MO
Rx1, XAG1
Sox2
A
B
C
D
E
F
G
H

FIG.8

***Figure 9. miR-15 and miR-16 are required to set the size of the organizer by limiting Nodal responsiveness***

**A-B.** Model showing the complementary asymmetries in miR-15 and miR-16 and Acvr2a distributions and model of the complementary asymmetries in early Wnt/beta-catenin signalling and miR-15 and miR-16 localization.

**C-D.** Effect of miR-15/16 functional inactivation with anti-miRNA reagents (14 ng; a 1:1 mix of anti-miR-16 and anti-miR-15 injected radially at the 4-cell stage) on embryonic organizer development (C) and on endogenous Nodal signalling (D). **C,** injection of anti-miR-15/16 leads to lateral expansion and upregulation of organizer markers (chordin, Admp, pintallavis, Xantivin). **D,** Loss of miR-15 and miR-16 increases Mix.2-lux transcription.

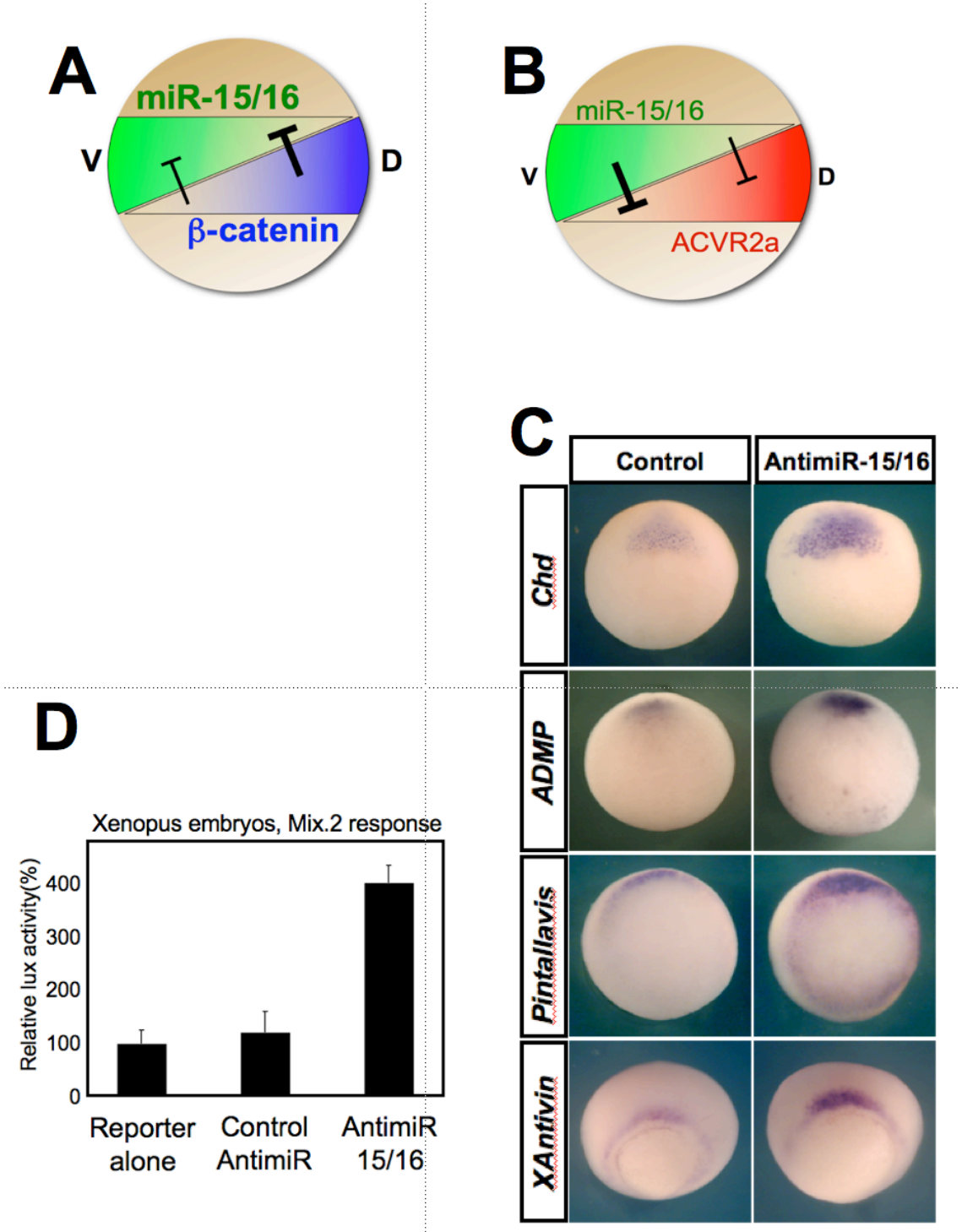
A
miR-15/16
V
D
β-catenin
B
miR-15/16
V
D
ACVR2a
C
Control
AntimiR-15/16
Chd
ADMP
Pintallavis
XAntivin
D
Xenopus embryos, Mix.2 response
Relative lux activity(%)
400
300
200
100
0
Reporter alone
Control AntimiR
AntimiR 15/16

FIG.9

***Figure 10. miR-15/16* confers robustness to head development by regulating ADMP/ACVR2a signaling**

**A-B.** Blockade of *miR-15/16* by injection of morpholino antisense oligonucleotides (*miR-15/16* MO, 100ng/embryo) induces mild head enlargement, as assayed by in situ hybridization for the markers *Rx1* and *XAG1*.

**C-D-E.** Injection of *miR-15/16* MO suppresses head formation in class III β-catenin depleted embryos (compare C and D). This is mimicked in (E) by overexpressing the *miR-15/16* target *ACVR2a* (100pg/embryo). Embryos were processed by in situ hybridization for the anterior markers *Rx1* and *XAG1*.

**F-G.** Loss of head structures due to increased ACVR2a in class III embryos is restored by co-injection of ADMP morpholino (ADMP MO, 40ng/embryo).

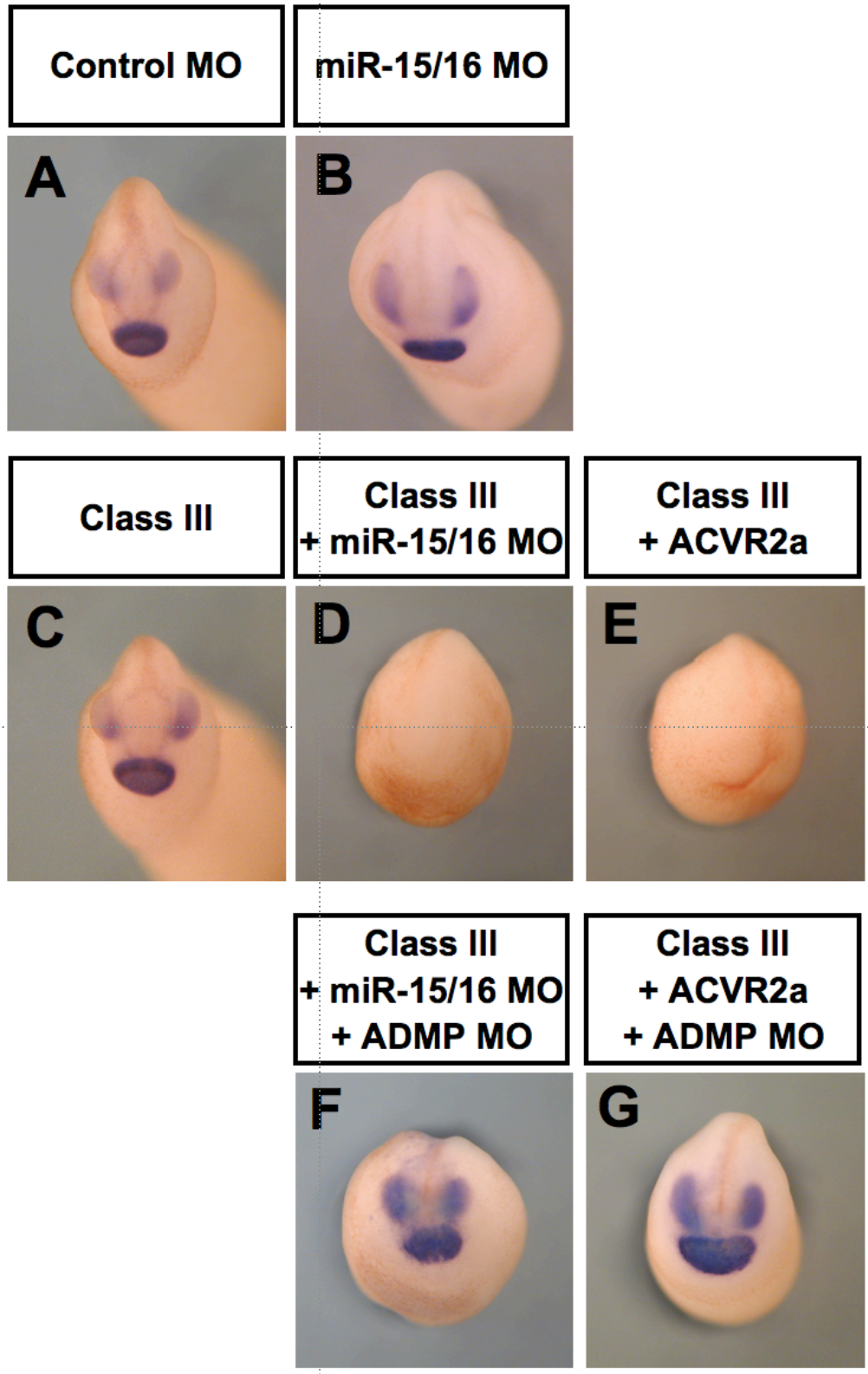
Control MO
miR-15/16 MO
A
B
Class III
Class III
+ miR-15/16 MO
Class III
+ ACVR2a
C
D
E
Class III
+ miR-15/16 MO
+ ADMP MO
Class III
+ ACVR2a
+ ADMP MO
F
G

FIG.10

***Figure 11. ADMP signals through ACVR2a.***

**This experiments were carried out by Luca Zacchigna.**

**A.** ADMP binds ACVR2a and Alk2 receptors, but not with BMPR2. Conditioned media from HEK293T cells expressing mature Myc-tagged cADMP were incubated with the extracellular domains of the indicated receptors fused to Fc and immobilized on proteinA-sepharose beads. Copurifying mature ADMP was visualized by anti-Myc immunoblotting.

**B.** ADMP activates Smad1/5 dependent transcription through ACVR2a. Human HepG2 cells were transfected with BMP-responsive *ID1*-luciferase reporter alone (Control) or with increasing doses of xADMP expression plasmid (10ng/cm$^2$, low; 40 ng/cm$^2$, high). Where indicated, cells were treated overnight with the type I BMP receptor kinase inhibitor Dorsomorphin (10μM), or cotransfected with Control- or ACVR2a-siRNA (50pmol/cm$^2$ each), mature *miR-15* (700pg/cm$^2$), or an ACVR2a expression plasmid (20ng/cm$^2$). Data are given as mean and SD.

**C.** ADMP overexpression (100pg/embryo) activates the BMP-responsive *ID1*-luciferase reporter in *Xenopus* ectodermal cells, but this is blocked by the concomitant injection of *dominant-negative ACVR2a* mRNA (DN-ACVR2a, 1ng/embryo). Embryos were injected at the 2-cell stage and harvested at gastrula.

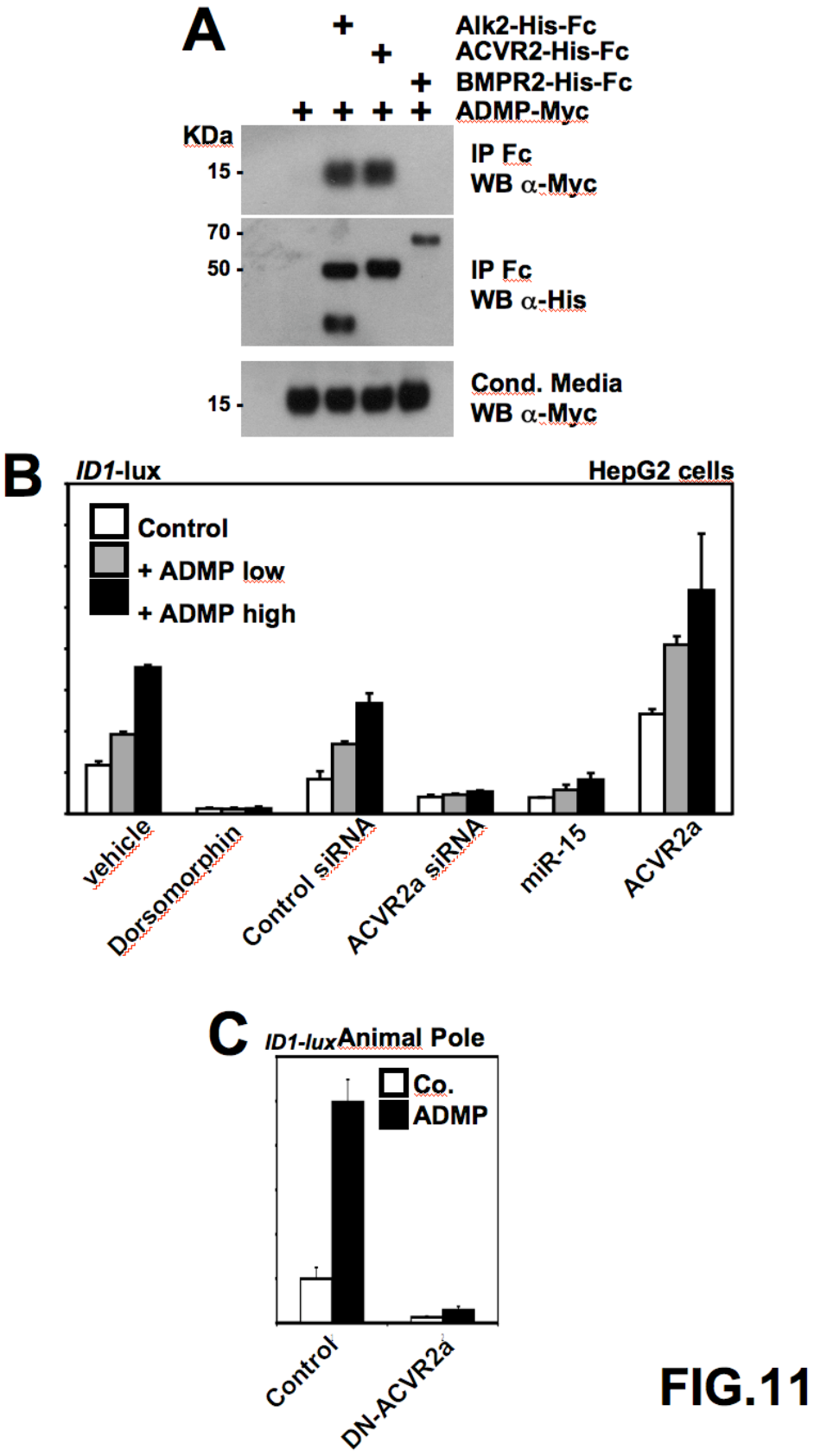
A
Alk2-His-Fc
ACVR2-His-Fc
BMPR2-His-Fc
ADMP-Myc
KDa
15
70
50
15
IP Fc
WB α-Myc
IP Fc
WB α-His
Cond. Media
WB α-Myc
B
ID1-lux
HepG2 cells
Control
+ ADMP low
+ ADMP high
vehicle
Dorsomorphin
Control siRNA
ACVR2a siRNA
miR-15
ACVR2a
C
ID1-luxAnimal Pole
Co.
ADMP
Control
DN-ACVR2a

FIG.11

***Figure 12. ADMP signals to the anterior endoderm region to restrain the expression of head inducers.***

**A-D.** Expression of *Cerberus* in anterior endodermal cells is negatively controlled by ADMP. 4-cell stage embryos were injected with the indicated antisense morpholinos (A and B) or with *ADMP* mRNA (D). At stage 11 embryos were fixed, removed of the blastocoel roof to reveal the underlying endoderm, and processed for in situ hybridization. Pictures of embryos were taken from the animal pole, dorsal side upward. Depletion of ADMP enhances (compare A and B) while ADMP overexpression inhibits (compare C and D) *Cerberus* expression.

**E-F.** Representative close-up pictures of the anterior endoderm region of *Xenopus* embryos stained for phosphorylated Smad1 (PSmad1). Embryos were injected with the indicated morpholinos, fixed at gastrula stage, and processed for immunohistochemistry with α-PSmad1 antibody. As control for the PSmad1 staining, inset in G shows a portion of anterior endoderm form a wild-type embryo stained with secondary antibody alone.

**G.** Quantitations of anterior endoderm nuclei positive for phosphorylated Smad1. Stained nuclei were manually counted in the dorsal endoderm of embryos stained as in (E and F). Data are mean and SD.

**H.** Embryos were injected with the ADMP-responsive reporter *ID1*-lux in dorsal blastomeres (C1) at 32-cell stage (Upper drawing). Targeting to anterior endoderm was confirmed at gastrula by coinjected *GFP* mRNA (Lower picture). Luciferase was determined on extracts from stage 10.5 embryos coinjected with Control or ADMP MO (Right panel).

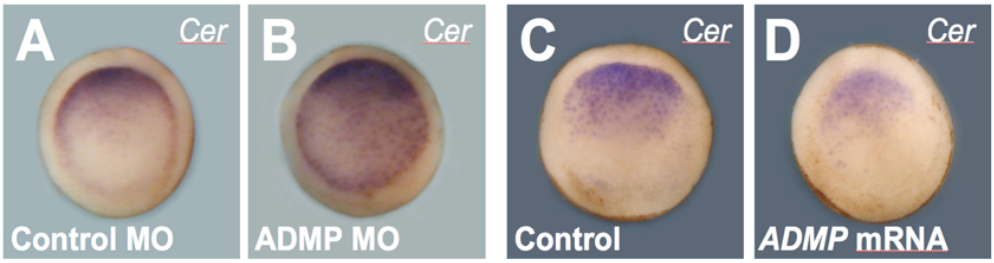
A
Cer
Control MO
B
Cer
ADMP MO
C
Cer
Control
D
Cer
ADMP mRNA

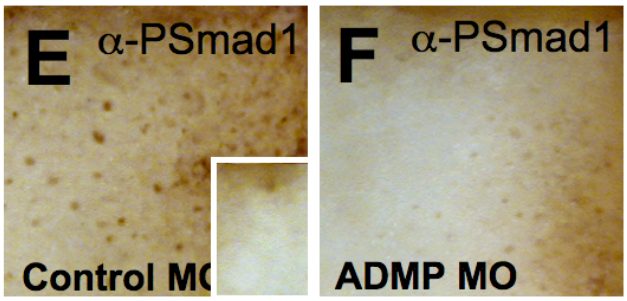
E
α-PSmad1
Control MO
F
α-PSmad1
ADMP MO

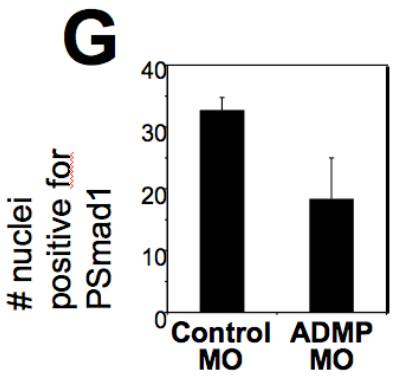
G
# nuclei positive for PSmad1
40
30
20
10
0
Control MO
ADMP MO

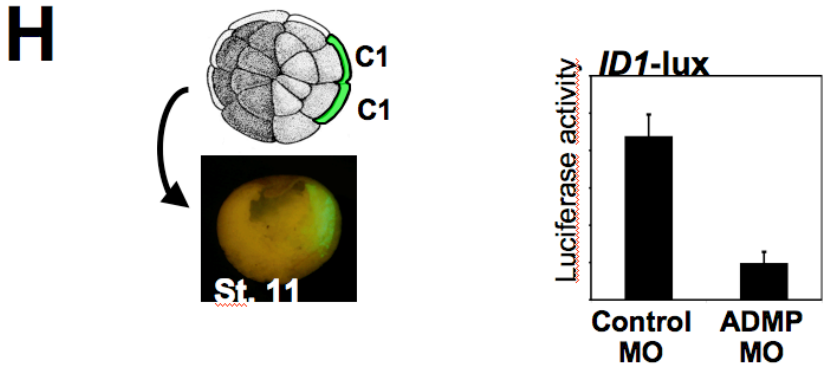
H
C1
C1
St. 11
ID1-lux
Luciferase activity
Control MO
ADMP MO

FIG.12

***Figure 13. Model of Organizer self-regulation by opposing Nodal and ADMP signaling.***

**A.** A simplified scheme illustrating the molecular interactions between Nodal, ADMP and ACVR2a (see text)

Left panel: in a *Xenopus* gastrula, the organizer is formed of dorsal mesodermal cells (blue), corresponding to the trunk organizer, and of the abutting anterior endoderm (yellow, expressing head-inducer molecules. D, dorsal; V, ventral.

Right panel: a scheme of the modeled molecular interplay between Nodal and ADMP in the boxed region of the left panel. Darker and lighter areas correspond to intracellular and extracellular spaces, respectively. N, Nodal ligand; A, ADMP ligand; Alk4 is a type I Nodal receptor; Alk2 is the type I ADMP receptor. Italicized names indicate gene transcription; *Cer* is used here as marker of head-organizer gene expression.

**B.** Overexpression of Xnr1 outcompetes ADMP from signaling through their shared receptor ACVR2a. Embryos were injected in the animal pole with the ADMP-responsive *ID1*-luciferase reporter alone (Control) or with combinations of *ADMP* (100pg/embryo), *Xnr1* (XYZpg/embryo) and *ACVR2a* mRNAs. Data are given as mean and SD.

**C.** ADMP does not outcompete Xnr1. Embryos were injected in the animal pole with the Nodal-responsive *Mix.2*-luciferase reporter alone (Control) or with combinations of the indicated mRNAs.

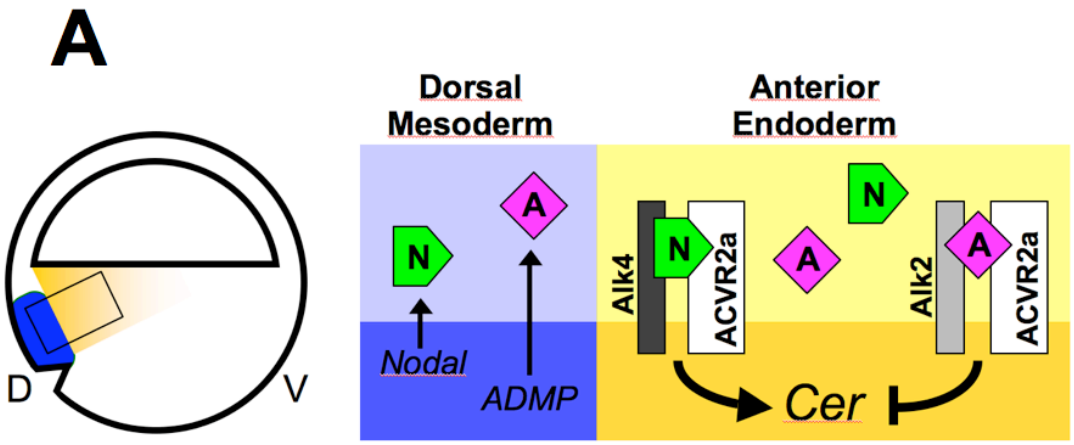
A
Dorsal Mesoderm
Anterior Endoderm
D
V
N
A
Nodal
ADMP
Alk4
ACVR2a
Alk2
Cer

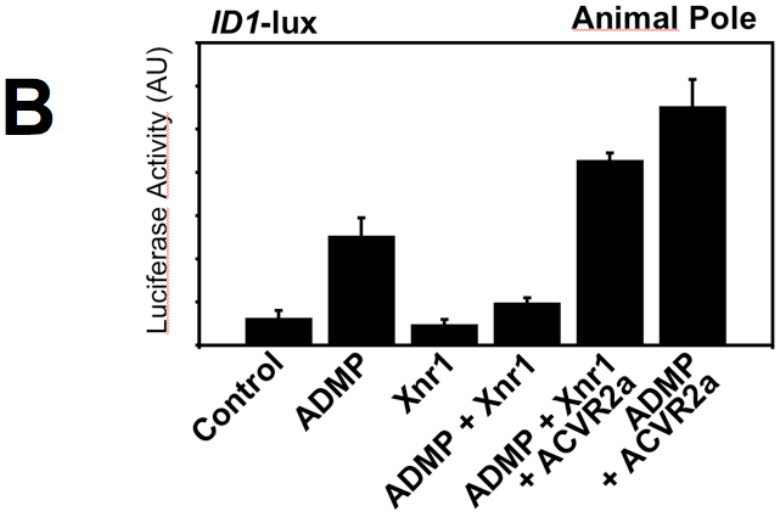
B
ID1-lux
Animal Pole
Luciferase Activity (AU)
Control
ADMP
Xnr1
ADMP + Xnr1
ADMP + Xnr1 + ACVR2a
ADMP + ACVR2a

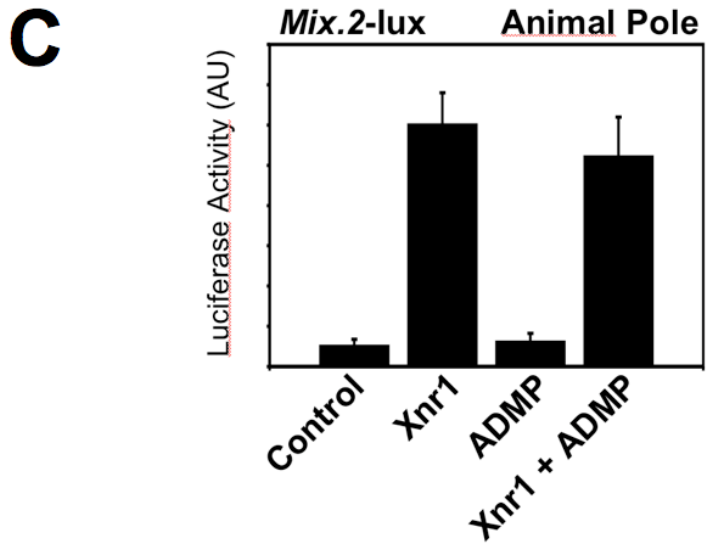
C
Mix.2-lux
Animal Pole
Luciferase Activity (AU)
Control
Xnr1
ADMP
Xnr1 + ADMP

FIG.13

***Figure 14. Cerberus facilitates ADMP signaling by relieving Nodal competition for ACVR2a.***

**A.** Cerberus protein production was introduced in the model depicted in Figure 13A. In the yellow area abutting the dorsal mesoderm, Nodal signals through ACVR2a and induces *Cerberus* expression. Secretion of Cerberus limits Nodal diffusion, enabling ADMP signaling in the gray area, where *Cerberus* expression is inhibited. Darker and lighter areas correspond to intracellular and extracellular spaces, respectively. N, Nodal ligand; A, ADMP ligand; C, Cerberus protein. Italicized names indicate gene transcription.

**B.** A model of the regulatory interactions between Nodal, ADMP, and Nodal antagonists in the Anterior Endoderm. Gray lines represent transcriptional events; black lines represent extracellular regulations between proteins.

**C-D-E-F-G-H.** Embryos were radially injected in the marginal zone at the 4-cell stage with the indicated combinations of antisense morpholino oligonucleotides and mRNAs (*ADMP*, 30pg/embryo; *CerS*, consisting of the pure Nodal inhibitory domain of Cerberus, 200pg/embryo; Cerberus+Lefty MOs, 60ng/embryo). Late gastrula-stage embryos were stained for the ADMP target *Sizzled*. Pictures were taken from the vegetal pole, dorsal side upward, on embryos bleached after in situ hybrdization. White dotted lines highlight the width of *Sizzled* expression domain.

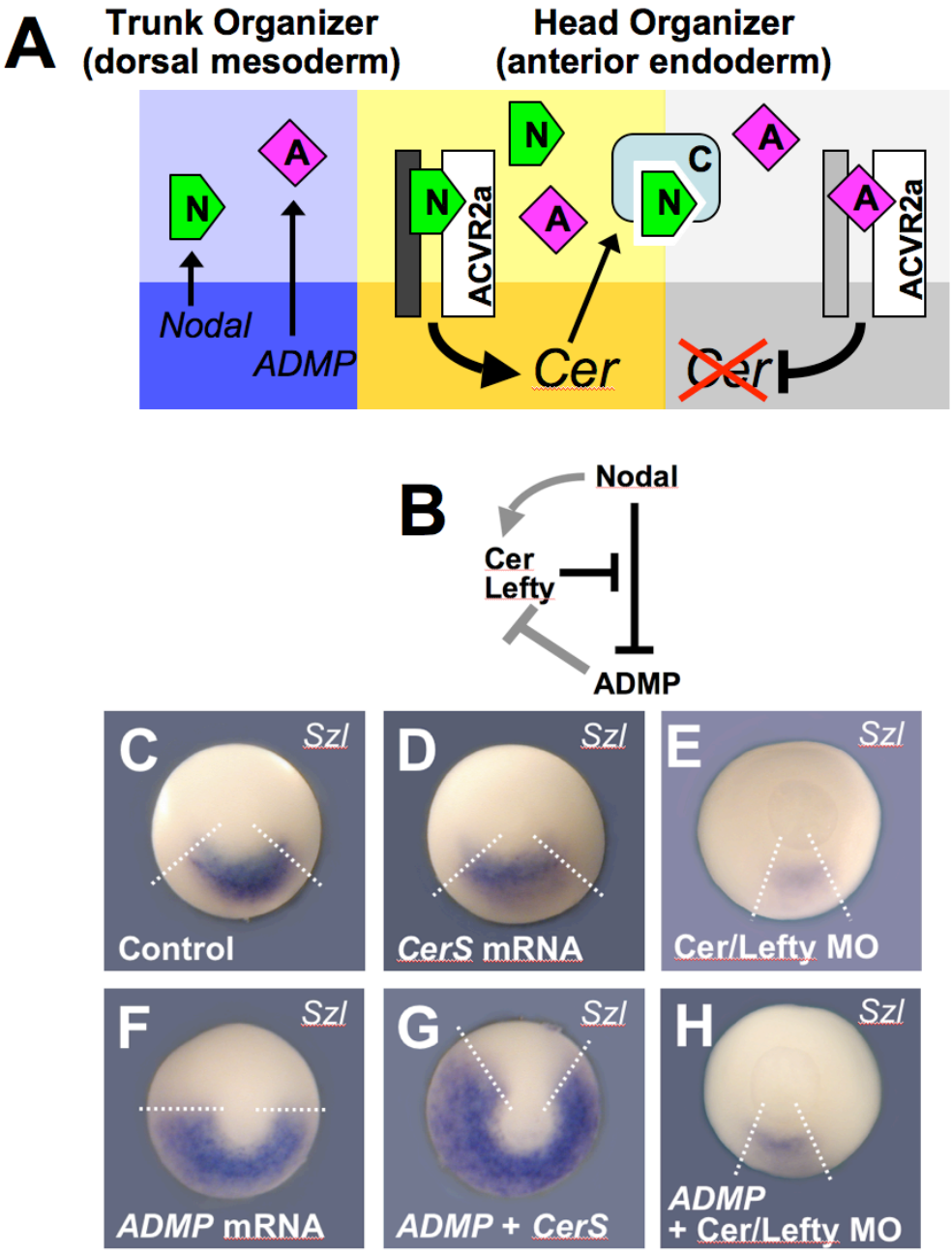
A
Trunk Organizer
(dorsal mesoderm)
Head Organizer
(anterior endoderm)
N
A
Nodal
ADMP
N
A
ACVR2a
Cer
C
N
A
ACVR2a
Cer
B
Nodal
Cer
Lefty
ADMP
C
Szl
Control
D
Szl
CerS mRNA
E
Szl
Cer/Lefty MO
F
Szl
ADMP mRNA
G
Szl
ADMP + CerS
H
Szl
ADMP
+ Cer/Lefty MO

FIG.14

***Figure 15. Validation of the model.***

**A.** same as in 14A, but the zig-zag serve as symbol of detachment between trunk and head organizer in explants of isolated anterior endoderm.

**B**. Anterior endoderm (Leading edge) explants injected with control or ADMP morpholinos, stained with Cerberus probe. T=0 are explants freshly isolated and immediately fixed. t=15 are explants cultured in media (20% Barth) for 15 minutes before fixation.

**C-D.** Anterior Endoderm explants dissected from early gastrula embryos injected with Control or ADMP morpholinos were transplanted into the blastocoel of wild-type recipient embryos (Einsteck grafts). Recipient embryos were allowed to develop until tadpole stage, when they were scored for the presence of ectopic head structures (white arrowheads, cement glands; black arrows, eyes). Percentage of induced heads: Control-MO injected grafts, 0/40; ADMP-MO injected grafts, 5/30.

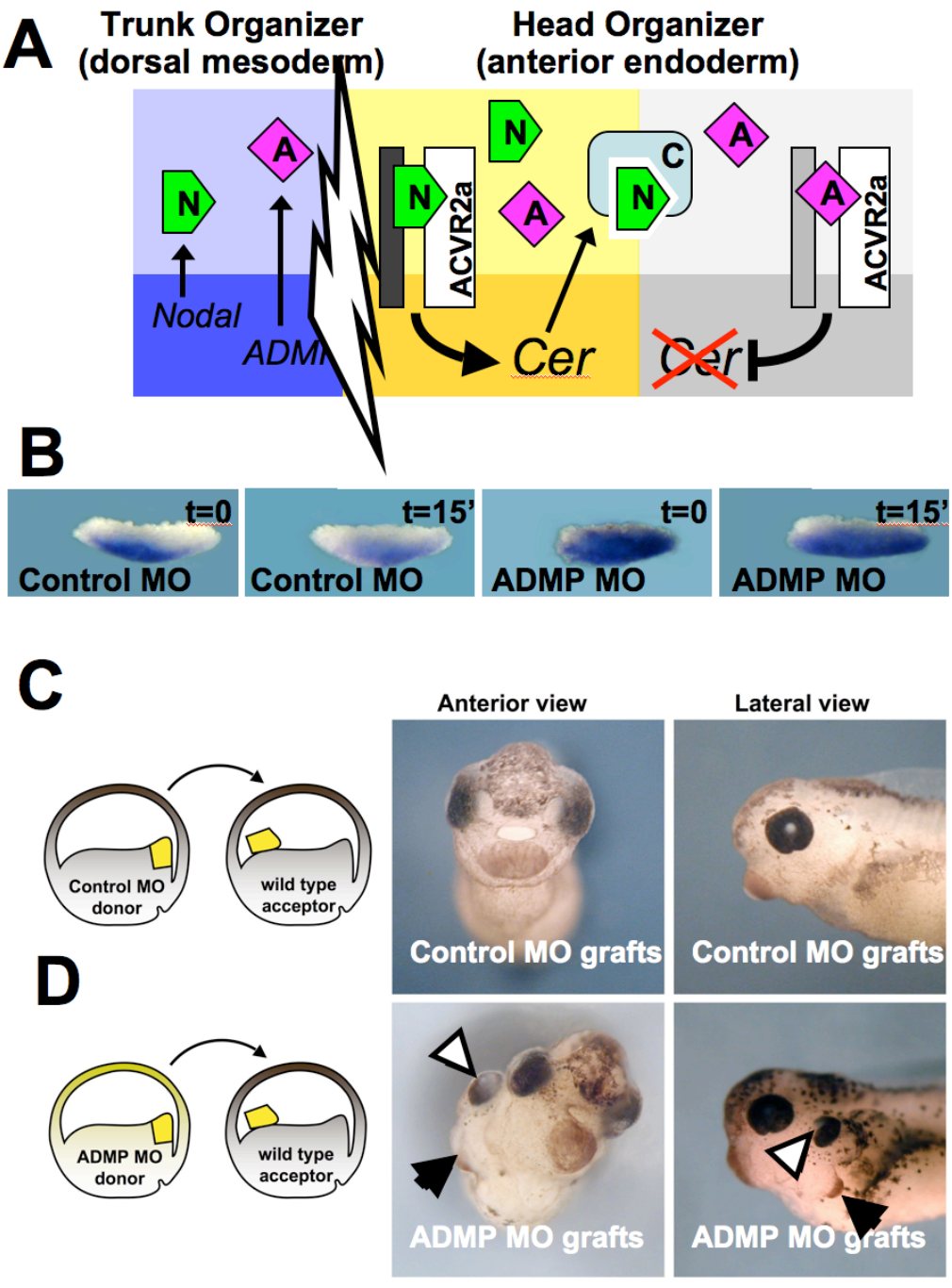
A
Trunk Organizer
(dorsal mesoderm)
Head Organizer
(anterior endoderm)
N
A
Nodal
ADMP
N
ACVR2a
N
A
C
N
A
Cer
A
ACVR2a
Cer
B
t=0
Control MO
t=15'
Control MO
t=0
ADMP MO
t=15'
ADMP MO
C
Control MO
donor
wild type
acceptor
D
ADMP MO
donor
wild type
acceptor
Anterior view
Lateral view
Control MO grafts
Control MO grafts
ADMP MO grafts
ADMP MO grafts

FIG.15

***Figure 16. A network assembled from simpler genetic circuits.***

**A.** This model incorporates 3 circuits: 1) in yellow, Nodal sustains its own expression and that one of its antagonists Cerberus and Lefty. 2) in pink, Nodal antagonists allows ADMP signaling; 3) in virtue of the double inhibition ADMP --| Cer/Lefty --| Nodal, ADMP sustains Nodal activity.

Gray lines represent transcriptional events; black lines represent extracellular regulations between proteins; dashed lines represent indirect events.

**B.** A scheme highlighting the two coherent and incoherent loops (in respect to expression of head inducers) through which β-catenin regulates Nodal and ADMP signaling.

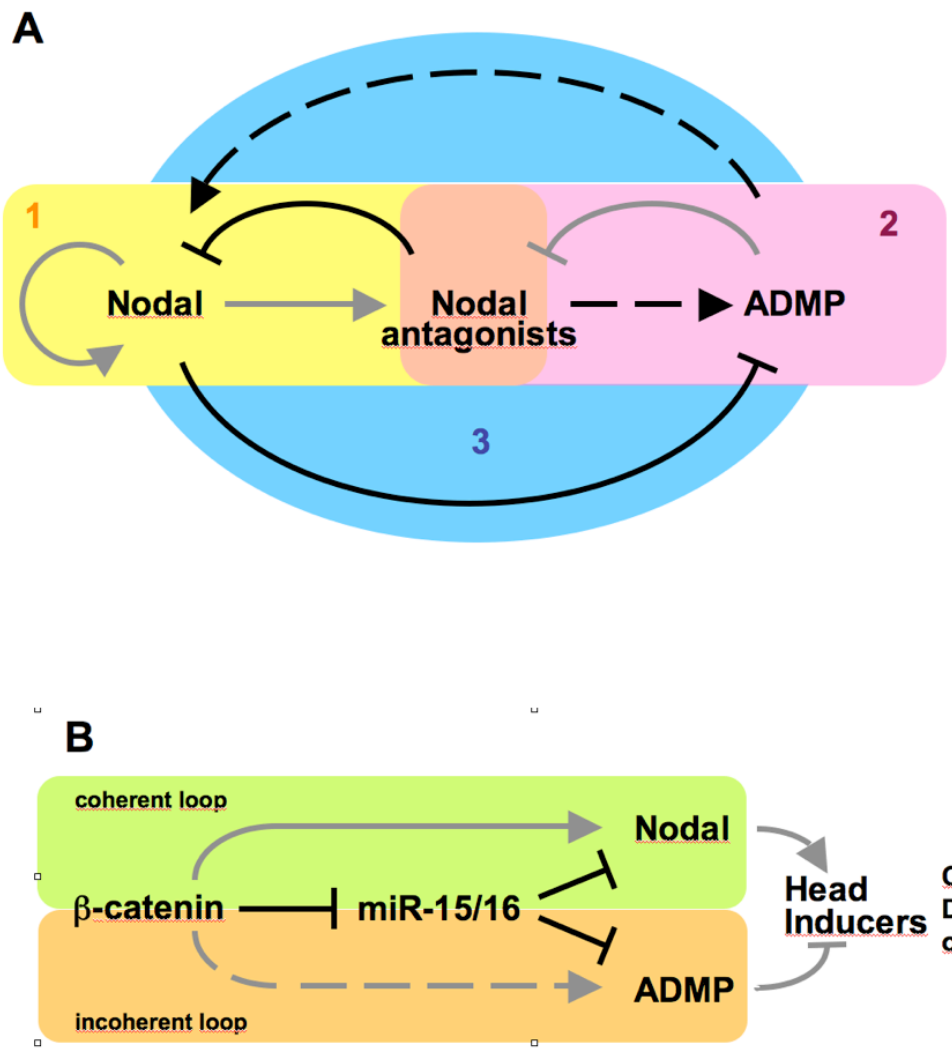
A
1
2
3
Nodal
Nodal antagonists
ADMP
B
coherent loop
Nodal
β-catenin
miR-15/16
Head Inducers
Cer
DKK1
others
ADMP
incoherent loop

FIG.16